Macrozooplankton Distribution and Feeding Ecology of Planktivorous Fish at the Barents Sea Polar Front

Frida Cnossen

UNIVERSITÉ CÔTE D'AZUR

Akvaplan niva

The Research Council of Norway

POLARFRONT
Ecosystem studies using novel autonomous technologies

Macrozooplankton Distribution and Feeding Ecology of Planktivorous Fish at the Barents Sea Polar Front.

2022 Graduate thesis project in fulfilment of the Master of Science degree in 'Science, Conservation, and Valorization of Marine Resources' at the Université Côte d'Azur in Nice, France.

Written by Frida Anneke Cnossen under the supervision of Paul E. Renaud (Akvaplan-niva).

EXECUTIVE SUMMARY

*T*he Barents Sea ecosystem is the most productive and diverse of all Arctic seas and is home to considerable commercial fisheries of global significance. It includes components of both the warmer more saline Atlantic and colder fresher Arctic compartments, while being controlled by a strong seasonal cycle. These two water masses meet at a boundary known as the Polar Front (PF), a biological hotspot with high ecological significance to a wide spectrum of organisms. Two key planktivorous fish species in the Barents Sea are capelin (*Mallotus villosus*), a subarctic specialized zooplankton feeder, and polar cod (*Boreogadus saida*), an Arctic generalist predator. These two species play strong roles in regulating the flow of energy from primary producers to top predators. Little is known, however, about the role of the PF in structuring macrozooplankton communities (copepods, krill, amphipods, gelatinous zooplankton, etc.) and its importance as a feeding ground for planktivorous fish. To analyse this, sampling was conducted along a transect of six stations across the PF near Hopen Trench in May 2022, a period with the highest primary production of the year. A traditional methodology of trawling and stomach content analysis was combined with a modern approach of broadband acoustic surveys to assess the macrozooplankton and fish communities, as well as the feeding by planktivorous fish across the PF.
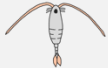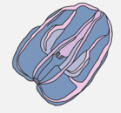
Two main co-occurring oceanographic features contributed to the biological observations in our study: the water mass (thermohaline) boundary imposed by the PF, and a more dynamic and seasonally occurring meltwater (MW) front from melting sea-ice. The PF acted as a barrier and was key in regulating the macrozooplankton distribution across the transect. Biological factors and local variations in water properties were mainly responsible for species abundances and patches of macrozooplankton organisms in the area. Temperature sensitivity and prey distribution regulated the distribution and feeding of capelin and polar cod, and stomach contents reflected macrozooplankton prey in the environment. Observed macrozooplankton accumulations near the PF provided a food source for planktivorous fish, as high feeding activity was observed just south of the PF. However, low abundances of herbivorous copepods further south were linked to high percentages of empty capelin stomachs. With ongoing climate change, the increase in zooplankton associated with a stronger AW influx (Atlantification) as well as the northward expansion of boreal species (borealization) will likely impact suitable zooplankton prey, competition, and predation in the PF area. This may have consequences for the persistence of important commercial stocks (e.g. Atlantic cod and haddock) that are dependent on these planktivorous fish species.

LEGEND

Acronyms

AW	Atlantic Water
ArW	Arctic Water
BSW	Barents Sea Water
MW	Meltwater
PF	Polar Front

Glossary of depictions

	Phytoplankton		Polar cod
	Copepod		Capelin
	Krill *Thysanoëssa* spp.		Herring
	Krill *Meganyctiphanes norvegica*		Atlantic cod
	Hyperiid amphipod *Themisto spp.*		Redfish
	Chaetognath		Haddock
	Sea angel		Seal
	Ctenophore		Orca
	Sea butterfly		Seagull
	Fish larva		Little auk
	Polar cod larva		Polar bear

CONTENTS

ABSTRACT

$\mathcal{T}$wo key fish species in the Barents Sea ecosystem are the Arctic polar cod (*Boreogadus saida*) and subarctic capelin (*Mallotus villosus*). These fish are predominantly planktivorous and play a key role in the transfer of energy-rich lipids from zooplankton to higher trophic levels, while being controlled by predation. The Polar Front (PF), defined as the interface between the warmer more saline Atlantic Water and the colder fresher Arctic Water, is primarily a passive front and was suspected to be a biological hotspot in the Barents Sea. Since an in-depth understanding on the influence of the PF on macrozooplankton and fish has been lacking, we tackled the questions on its role in structuring macrozooplankton communities and its importance as a feeding ground to planktivorous fish. Two main co-occurring oceanographic features dominated the hydrological regime in the area, namely the PF and a seasonally occurring meltwater (MW) front. Our findings highlight that 1) the PF acts as a sharp biological boundary and regulates latitudinal macrozooplankton distribution, while both hydrographical and biological factors affect species-specific abundances, patchiness, and aggregations near the PF, and 2) sensitivity to temperature and prey distribution influence the distribution and feeding patterns of capelin and polar cod, and both fish species were able to exploit food sources south of the PF. We also shed light how biophysical interactions at the PF might be impacted during the Arctic ecosystems evolution in a progressing Atlantification scenario.

Keywords: Barents Sea Polar Front, macrozooplankton, planktivorous fish, capelin, polar cod, species distribution, feeding ecology, dietary structure

1   INTRODUCTION

1.1   The Barents Sea ecosystem

𝒯he Barents Sea is the largest (± 1.6 x 10^6 km^2) and the deepest (mean depth ~230 m, max. ~400 m) among the pan-Arctic shelf seas (Carmack et al., 2006). The sea is connected to the Norwegian and Greenland Seas in the west, the Arctic Ocean in the north, and the Kara Sea in the east. Despite it being located at high latitude, it is characterized by a relatively high biological productivity. The marine ecosystem is recognized for some of the world's largest demersal fish stocks, such as Atlantic cod (*Gadus morhua* Linnaeus, 1758), and haddock (*Melanogrammus aeglefinus* Linnaeus, 1758), as well as pelagic stocks including capelin (*Mallotus villosus* Müller, 1776), and it further serves as a nursery ground for herring (*Clupea harengus* Linnaeus, 1758). These stocks have sustained fisheries with a long-term average of 1.5-3 million tons of catch annually over the past few decades (Hunt et al., 2013; ICES 2019).

The biological system is adapted to a strong seasonal cycle with extreme variations in light, and controlled by a range of physical oceanographic conditions, including variations in temperature, currents, and ice coverage (Sakshaug et al., 2009). Many of these conditions within the Barents Sea are largely determined by the three dominating water masses: Coastal Water, (North-)Atlantic Water (AW), and Arctic Water (ArW), which are linked to the Norwegian Coastal Current, the (North-)Atlantic Current, and the Arctic Current, respectively (Loeng, 1991). The properties of these water masses make the Barents Sea a biogeographical transition zone between the warmer boreal south and a colder Arctic north (Fossheim et al., 2015).

The ecosystem dynamics of the Barents Sea are regulated through several different mechanisms, including 1) bottom-up processes from producers sustaining higher trophic levels (Dalpadado et al., 2014), 2) top-down processes (trophic cascades) from top predators altering the abundance, biomass, or productivity of lower trophic levels (Pace et al., 1999) and 3) 'wasp-waist' regulation where a few intermediate species pass most of the energy from lower to higher trophic levels (bottom-up), while their feeding has top-down effects on zooplankton and phytoplankton (*Figure 1*). The last is typical for productive ecosystems including the Barents Sea, where one or a few small pelagic planktivorous fish, here mainly capelin (Yaragina and Dolgov, 2009), occupy this intermediate trophic level (Cury et al., 2000). Drastic impacts on the abundance of these small pelagic fish (e.g. from overfishing, climate change) have been shown to alter biomass of lower and higher trophic levels, (Loeng & Drinkwater, 2007; Yaragina & Dolgov, 2009), and can affect spatial dynamics (e.g. fish migration patterns) (Cury et al., 2000). Nevertheless, it is usually a changing combination of these three controlling mechanisms that regulates the marine ecosystem, depending on its state, diversity, fisheries impact, and changing environmental conditions (Cury et al., 2000; Frank et al., 2007).
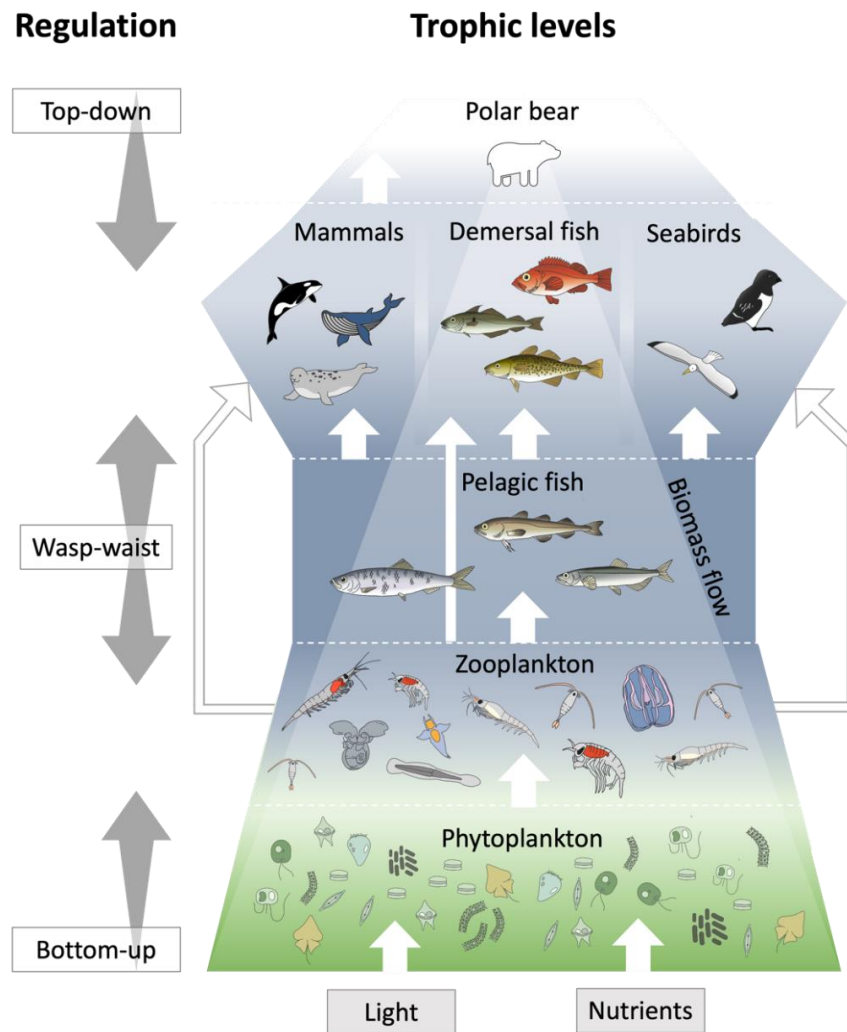
Figure 1*: Conceptual understanding of the Barents Sea ecosystem trophic levels and modes of regulation. The biomass flow across trophic levels is depicted by the pyramidical shape, and the overall shape of the figure corresponds to species diversity. Illustration: Frida Cnossen. Adapted from Yaragina & Dolgov (2009).*

Pelagic primary production is a prominent component in fuelling Arctic marine ecosystems, including the Barents Sea. Photosynthetic organisms synthesize organic matter from inorganic compounds using solar energy. They are crucial in driving secondary production, which forms the prime food source for all higher trophic levels, such as fish, sea birds, marine mammals, benthic communities, and other types of zooplankton (Daase et al., 2021). The Arctic ecosystem is said to be a lipid-driven food chain, as many Arctic zooplankton species build up stores of polyunsaturated fatty acids generated from carbohydrates, proteins, and fatty acid precursors by phytoplankton. This is typically considered as an adaptation to the cold and high latitude climates due to the high energy content stored within these lipids. They form a valuable food source for higher trophic levels, and lead to large annual migrations of predators to the Arctic during the summer when secondary production reaches its peak (Falk-Petersen et al., 1990; Scott et al., 1999; Lee et al., 2006; Daase et al., 2021).

1.2   Arctic and Atlantic Spring bloom

A strong seasonal cycle tightly controls the timeframe in which primary production occurs in the Barents Sea. That is to say, north of the Polar Circle, during winter and summer, the sun does not rise or set above or below the horizon for at least one 24-hour cycle, respectively (Sakshaug, 2004; Daase et al., 2021). The duration of these periods increases with latitude, which consequently decreases the amplitude of the pelagic primary production cycle (Leu et al., 2011). Additionally, ice and snow coverage limit the amount of light that is able to reach the water column (Perovich et al., 1998; Mundy et al., 2007). The freezing and melting of sea-ice and solar heating affect water column stratification, which impacts mixing processes in the water column (Sakshaug, 2004; Eriksen et al., 2017). Phytoplankton blooms in the AW and ArW are initialized by different physical conditions, and 'new' carbon production in the AW can be as high as 90 g C m^{-2} yr^{-1}, whereas in ArW this is typically less than 40 g C m^{-2} yr^{-1} (Sakshaug & Slagstad, 1992).

In the ArW of the Barents Sea, a spring bloom is triggered by the stabilization of the water column from ice melting within the seasonal sea-ice zone (Wassmann et al., 2006). During the winter, the properties of ArW are relatively constant over a depth of 150 m. However, the onset of ice melting during spring and summer causes a strong stratification of the water column, leaving a stable layer of melting water (T > 0 ºC) with low salinity (31.0 – 34.2 PSU) of 5-20m thickness on top of the rest of the water column (Loeng, 1991). This meltwater (MW) layer results in a sharp thermo- and halocline. Stabilization of the water column traps nutrients in the euphotic zone, and the exposed surface allows light to penetrate into the water column. This leads to intense algal blooms along the marginal ice zone (Engelsen et al., 2002; Sakshaug et al., 1994; Sakshaug, 2004), followed by a bloom of secondary producers, until nutrients and food availability are depleted. During winter, when winds and cooling temperatures trigger ice formation, the resulting brine rejection causes the water column stratification to be disrupted. This allows for nutrient replenishment through vertical mixing processes, where nutrients from greater depths are being transported back to the euphotic layer, making the annual cycle complete (Loeng, 1991).

While sea-ice melt triggers the ArW spring bloom, stabilization of the AW column occurs through thermocline formation when the sun heats the surface layer (Sakshaug, 2004). The stratification of AW tends to be weaker and develops more slowly compared to ArW due to its greater susceptibility to being disrupted by winds. This wind-induced mixing occurs over 40-60 m depths as a result of recurrent atmospheric depressions, and causes pulses of nutrients from below with an approximate one-week rhythm (Sakshaug et al., 1994; 1997). However, the effect of the wind on vertical mixing becomes less as the thermally induced stratification increases during the summer (Sakshaug & Slagstad, 1992). The onset of a pelagic bloom in AW therefore occurs later than in the ArW (Sakshaug, 1997). Nevertheless, the annual primary production can be twice as high in AW compared to ArW, and the intensity

and duration of the pelagic bloom are greater than in ArW. This can be explained by the deeper mixing events resulting in greater nutrient availability, as well as the wind replenishing the surface layers with nutrient-rich water from the depth (Sakshaug & Slagstad, 1992).

1.3   Secondary production Barents Sea

*Z*ooplankton are the main route of biomass transfer between the primary producers and pelagic carnivores, and eventually the top predators (Eiane & Tande, 2009). In the Barents Sea, the annual biomass production of zooplankton undergoes large seasonal and interannual variations. The intense phytoplankton spring bloom, which is closely associated with the receding ice edge, produces copious food for herbivorous zooplankton. (Falk-Petersen et al., 2000). This is associated with an efficient energy flux, as lipid levels increase from 10-20% of dry mass in phytoplankton to 50-70% of dry mass in herbivorous zooplankton (Falk-Petersen et al., 1990). This energy transformation is an important step for transferring high-energy fatty acids to the top predators within one season (Falk-Petersen et al., 1990, 2009). In addition, a significant portion of zooplankton is also advected with the Atlantic Current into the Barents Sea (Edvardsen et al., 2003; Wassmann et al., 2019). The advective zooplankton biomass flux experiences great seasonal and interannual changes, (Skjoldal et al., 1987; Wassmann et al., 2006), and is higher during warm years when the magnitude of AW influx is stronger (Skjoldal et al., 1992; Sakshaug et al., 1994).

The Barents Sea has rich mesozooplankton (0.2 – 2mm) and macrozooplankton (> 2mm) communities, among which copepods, euphausiids, and amphipods form important prey items for many planktivorous fish (Eiane & Tande, 2009). The zooplankton species in the Barents Sea can be classified as Arctic, Atlantic (boreal), or boreal-arctic/Arctic-boreal (mixed), depending on their associations with the different water masses occurring in the Barents Sea, and can also be classified based on their feeding modes (Søreide et al., 2003) (*Table 5,* Appendix II).

Copepods

Copepods form the predominant group among the herbivorous mesozooplankton and account for 70-90% of the mesozooplankton biomass in the Barents Sea (Tande, 1991). Among these, *Calanus* spp. are particularly common in the Barents Sea. The *Calanus* genus includes three key species that have gained much attention for studying their ecology in the Barents Sea: *Calanus finmarchius* (Gunnerus, 1770)*, Calanus glacialis* (Jaschnov, 1955)*,* and *Calanus hyperboreus* (Krøyer, 1838)*.* Although all three species can be observed throughout many parts of the Barents Sea, *C. finmarchius* occurs generally in AW, whereas *C. glacialis* and *C. hyperboreus* mainly occur in ArW. These species have physiological and life cycle adaptations suited to their main areas of distribution and strong seasonal regime (Falk-Petersen et al. 2009). Life-cycle duration generally increases with latitude as water

temperature decreases and food supply becomes less predictable (Daase et al., 2021). The three *Calanus* species have the ability to accumulate large lipid reserves during periods of high food availability, especially at higher latitudes, which can provide much energy to higher trophic levels (Falk-Petersen et al., 2009). These energy reserves also sustain them during the winter periods when food availability is low, including when they descend to deeper waters and enter diapause until the next spring bloom (Hirche & Kattner, 1993; Søreide et al., 2010). Long life cycles and late reproductive maturity are a common feature of high latitude species. This is thought to result from the seasonal resource limitation, making food from primary production often limited for herbivorous zooplankton (Søreide et al., 2003; Leu et al., 2011). Other commonly found large copepod species that generally occupy deeper waters in the Barents Sea are the omnivorous *Metridia longa* (Lubbock, 1854), as well as the carnivorous *Paraeuchaeta norvegica* (Boeck, 1872) and *Paraeuchaeta glacialis* (Hansen, 1886). *M. longa* can be particularly abundant after the spring phytoplankton bloom, and *Paraeuchaeta* spp. can prey intensively on overwintering copepods (Eiane & Tande, 2009).

Euphausiids

Euphausiids, more commonly known as krill, are the second most numerically abundant group of zooplankton occurring in the Barents Sea. Among the eight species recorded in Arctic and subarctic waters, four species regularly appear in the Barents Sea and are mostly associated with AW (Eiane & Tande, 2009; Eriksen et al., 2017). This includes three species of the genus *Thysanoëssa*, namely *Thysanoëssa inermis* (Krøyer, 1846), *Thysanoëssa raschii* (Sars, 1864), and *Thysanoëssa longicaudata* (Krøyer, 1846)*. The boreal-arctic species *T. inermis* is the most abundant in the Barents Sea, and consists of reproducing populations in the southern and central parts, but also some populations that are advected by currents from the Norwegian Sea. *T. raschii* has a distribution in the shallower north-easterly parts of the Barents Sea, as it prefers colder, less-saline water (Eiane & Tande, 2009; Zhukova et al., 2009). The fourth species, *Meganyctiphanes norvegica* (Sars, 1857) is the largest euphausiid species in the Barents Sea, but rarely dominates in plankton samples. *T. longicaudata* and *M. norvegica* are boreal species with main spawning grounds in the Norwegian Sea, and their abundance depends upon advection by the Atlantic current (Dalpadado & Skjoldal, 1991; Orlova et al., 2015). The greatest abundances of these euphausiids can be found in the AW (Søreide et al., 2003), and lower abundances in the ArW (Orlova et al., 2015; Eriksen et al., 2016). Advective processes often influence species composition and distribution, although this may vary on a regional scale (Wassmann et al., 2006; Orlova et al., 2015). Additionally, the abundance of euphausiids can be strongly affected by predation pressure (Orlova et al., 2013).

Amphipods

Amphipods are the third most abundant zooplankton group in the Barents Sea, far exceeded by copepods and krill, yet they constitute an important part of the diet of several planktivorous fish (Dalpadado, Borkner, Bogstad, & Mehl, 2001; Eriksen et al., 2020). Within

the order of pelagic amphipods, hyperiids of the genus *Themisto* dominate in the Barents Sea. This includes the Arctic species *Themisto libellula* (Lichtenstein in Mandt, 1822)*,* as well as the boreal-arctic species *Themisto abyssorum* (Boeck, 1871)*. T. libellula* is a key species within the Arctic food web and occurs largely in the ArW (Dalpadado, Borkner, Bogstad, & Mehl, 2001). It is heavily preyed upon by fish species including polar cod, as well as other animals foraging in closely along the ice edge. *T. abyssorum,* on the other hand, is an important prey item for animals in the Atlantic and boreal waters (Dalpadado et al., 2012).

Other forms of zooplankton

Various other zooplankton species can be abundant at times in the Barents Sea, such as comb jellies (ctenophores), arrow worms (chaetognaths), cnidarians, and mollusks (particularly pteropods). A collective trait among these phyla is their disproportionally high water content, hence they are often referred to as gelatinous zooplankton. Most of these species exhibit either carnivorous or omnivorous dietary strategies (Søreide et al., 2003; Eiane & Tande, 2009). A list of species included in this study with their corresponding water mass distribution and feeding mode can be found in *Table 5* (Appendix II).

1.4   Planktivorous fish in the Barents Sea

*W*asp-waist regulation by planktivorous fish, as introduced earlier, has been shown to have a strong effect in the Barents Sea, with a few planktivorous fish species forming a crucial link between secondary production and higher trophic levels, including top predators (Yaragina & Dolgov, 2009). Two key planktivorous fish species in the Arctic marine food web are polar cod (*Boreogadus saida* Lepechin, 1774) and capelin (*Mallotus villosus* Müller, 1776), which have different associations with the water masses occurring in the Barents Sea (*Figure 2*). On the one hand, polar cod is an endemic high-Arctic species, known to survive in sub-zero temperatures due to the presence of anti-freeze proteins circulating in the blood (Osuga & Feeney, 1978). On the other hand, capelin is an important commercial stock in the Barents Sea with a more restricted sub-Arctic distribution (Gjøsæter, 1998). Though higher temperatures up till 3-4 ºC make growth and survival of polar cod more favorable, it typically occupies waters below its optimal temperature due to its specialization to cold water and to reduce competition (Hop & Gjøsæter, 2013). The distribution of capelin is more variable than polar cod, as warm years causes capelin to extend further northwards, whereas cold years contracts capelin populations. Increased expansion towards the northeastern areas may also take place when capelin occur in high abundances, and when the zooplankton production needs to be utilized over a larger area due to the higher food demand (Gjøsæter, 2000; Orlova et al., 2010; Ingvaldsen & Gjøsæter, 2013).
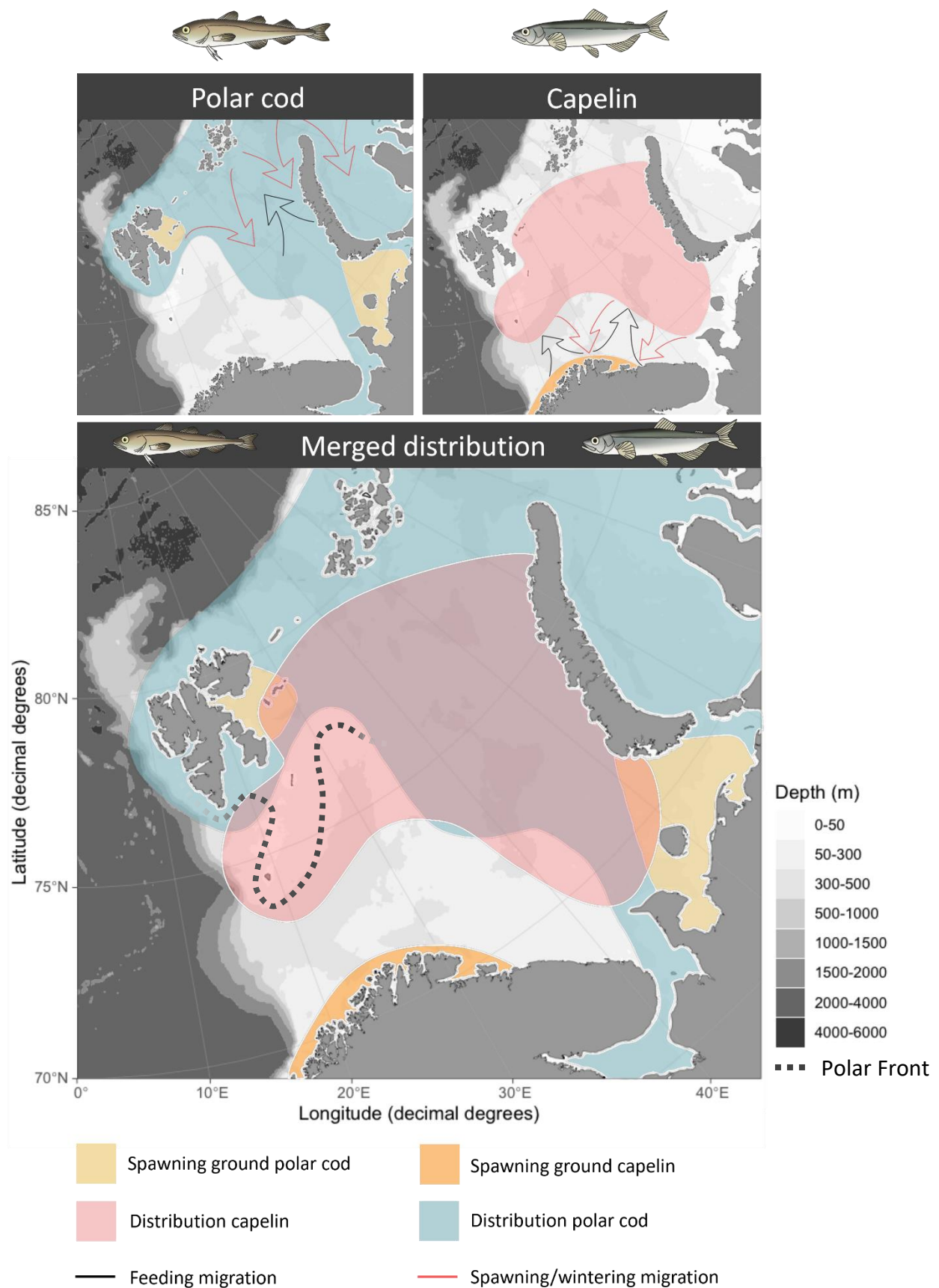
Figure 2: *distributions of polar cod and capelin and their annual migration patterns. Illustration: Frida Cnossen. Adapted from Aune et al. (2021), Gjøsæter et al. (2012), and Skaret (2020).*

While polar cod and capelin have an overlapping distribution in the southern and eastern parts of the Barents Sea, they also have considerable dietary overlap (*Figure 3*), which may lead to interspecies competition in regions where they both occur (Orlova et al., 2009; Hop & Gjøsæter, 2013). Both capelin and polar cod form large schools (Welch et al., 1993; Gjøsæter, 1998) that have the ability to deplete zooplankton locally, thus regulating its density and biomass through predation pressure (Hop et al., 1997). Three groups of zooplankton as described above (i.e. copepods, euphausiids, and amphipods) make up a large part of their diet and constitute an important high-energy source for higher trophic levels (Ajiad & Gjøsæter, 1990; Dalpadado, Borkner, Bogstad, & Mehl, 2001; Wassmann et al., 2006; Hop & Gjøsæter, 2013; Eriksen et al., 2020). They both feed on calanoid copepods, but the main prey item for polar cod are hyperiid amphipods, whereas euphausiids constitute a large part of the diet of capelin (Eriksen et al., 2020). Other food items also frequently found in the stomachs include various forms of gelatinous zooplankton (e.g. chaetognaths, cnidarians, pteropods, and appendicularians), though they constitute a lesser nutritional value (Orlova et al., 2009).
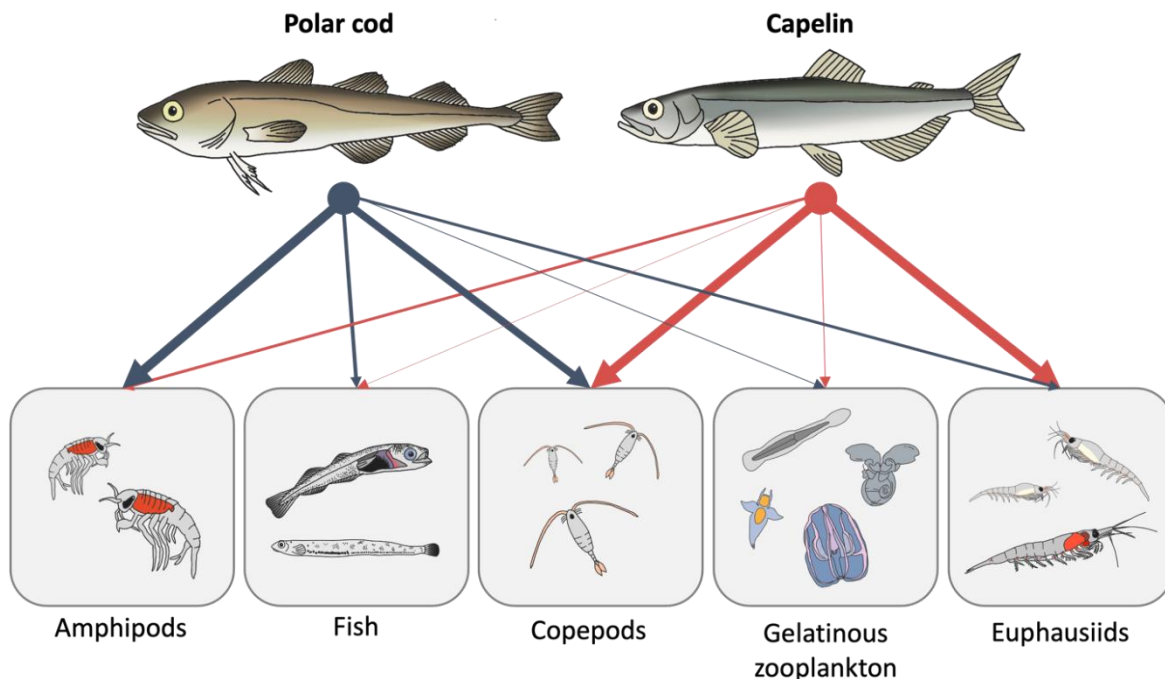
Figure 3: *General overview of the feeding ecology of polar cod and capelin, with arrow thickness corresponding to the magnitude of prey ingestion. Illustration: Frida Cnossen. Adapted from Eriksen et al. (2020).*

Polar cod

Polar cod is considered a generalist planktivorous feeder (Renaud et al., 2012), and mainly consumes larger forms of zooplankton as well as ice-associated fauna (Lønne & Gulliksen, 1989). Adult fish feed more in the near-bottom layers of the water column (Orlova et al., 2009). Despite the limited understanding of its preferred habitat, it is generally assumed that polar cod is sympagic (i.e. lives in association with the ice) at young stages; spawning happens underneath the ice from November to March, and young polar cod are frequently

found residing within ice cracks and brine channels where they are sheltered from predators (Hop & Gjøsæter, 2013; Huserbråten et al., 2019). Juvenile and adults are both found to inhabit benthic and pelagic habitats in open waters and in the water column underneath the ice (Hop et al., 1997; Geoffroy et al., 2011). The foraging behaviour is often influenced by local prey availability as well as mechanical and behavioral capabilities of the fish. That is to say, copepods form the main source of food for fish larvae and juveniles, whereas larger prey (e.g. amphipods, teleosts) become more important as fish grow (*Figure 4*) (Ajiad & Gjøsæter, 1990; Renaud et al., 2012). In March-May, post-spawning polar cod have been found to migrate from the central regions towards the ice edge for feeding, where they follow the ice edge as it recedes northwards (Aune et al., 2021).

Capelin

Capelin is a key species and specialized plankton feeder in the Barents Sea, while it also serves as a critical food source for Atlantic cod (Gjøsæter, 1998; Hop & Gjøsæter, 2013). It performs seasonal migrations towards the central and northern parts of the Barents Sea where it feeds on the zooplankton blooms during the Arctic summer (Gjøsæter, 1998). The annual feeding migration may also be an adaptation to avoid predation by Atlantic cod, its main predator (Hop & Gjøsæter, 2013). They tend to follow the bloom along the marginal ice zone by establishing the "capelin front", while rapidly depleting the available food in several days (Hassel et al., 1991). Mature capelin tend to migrate farther north than immature individuals (Olsen et al., 2010). The feeding is also dependent upon other factors, such as fish length and spatial and seasonal prey availability. Copepods constitute a larger part of the diet in smaller capelin (<10-12 cm), whereas euphausiids become a key dietary item as capelin grows (>12 cm) (*Figure 4*) (Dalpadado & Mowbray, 2013). Euphausiids can dominate the diet in February when capelin feed near the coastline, whereas *Calanus* spp., euphausiids, and amphipods peak during the summer months in July-October when zooplankton blooms. After the feeding season, capelin migrate back towards their spawning grounds along the Norwegian coast, and high energy from grazing on lipid-rich zooplankton is being funneled towards higher trophic levels including Atlantic cod, seabirds, and mammals (Gjøsæter, 1998; Sakshaug et al., 1994; Wassmann et al., 2006).
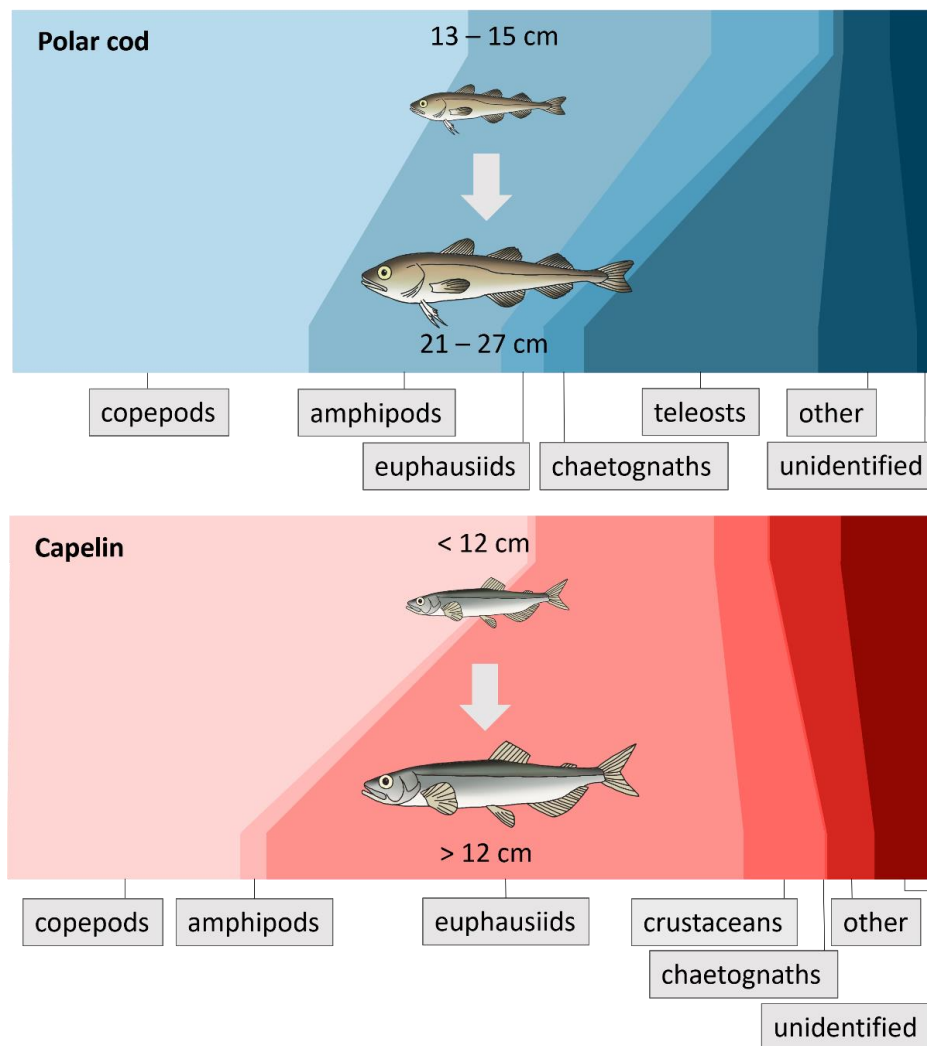
Figure 4: *Change in prey composition versus fish growth of polar cod (top) and capelin (bottom). Colour shades correspond to the different prey item groups. Illustration: Frida Cnossen. Adapted from Hop & Gjøsæter (2013).*

1.5   The Polar Front

*T*he AW and ArW masses in the Barents Sea meet at the Polar Front (PF) (*Figure 5*), where the marked ecological gradient has strong influences on the distribution of stocks and processes of many ecosystem components. Zooplankton and fish distributions are also impacted by the positions of the two main water masses (see above). The greater density resulting from the higher salinity of the AW causes it to descend underneath the less dense ArW (Loeng, 1991; Harris et al., 1998). The geographical location of the PF location is tightly coupled with the bathymetry and typically located around the 200m isobath. This makes the boundary more distinct in the west around Spitsbergen Bank, Hopen Deep, and Central Bank, compared to the shallower eastern Barents Sea. West of 32° E, both salinity and temperature gradients comprise the PF, whereas east of 32° E, the PF splits into a northern salinity branch and a southern temperature branch because of the weaker topographic constraint. These

branches go along with a more pronounced spatial and interannual variability than in the west (Oziel et al., 2016; Barton et al., 2018).
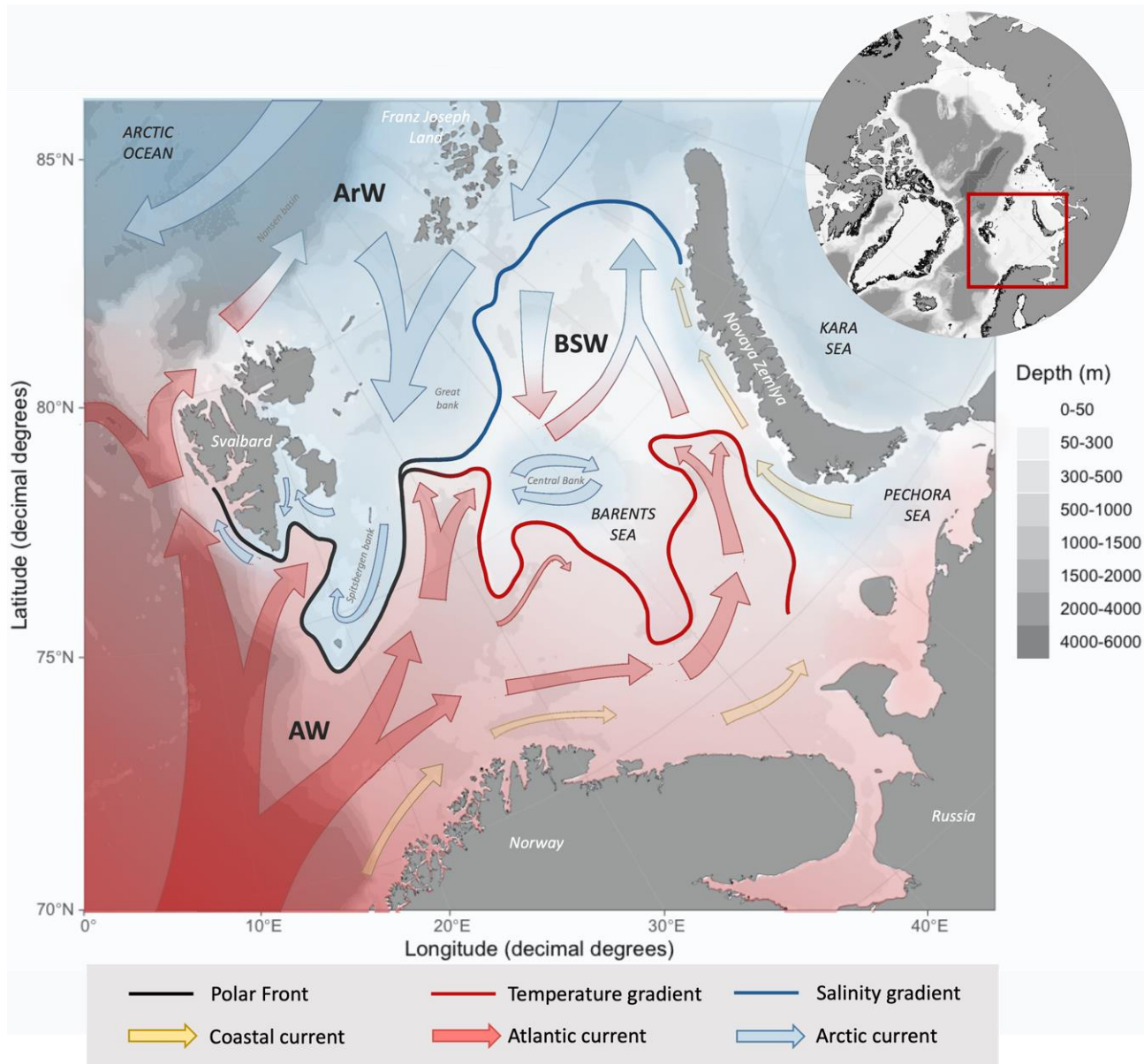
Figure 5: *overview of the Barents Sea currents, water masses and main position of the PF. Illustration: Frida Cnossen. Adapted from Gjøsæter et al. (2020) & Oziel et al. (2016)*

The PF is also the approximate location of the southern border of seasonal sea-ice (except for very cold years) (Loeng, 1991; Harris et al., 1998), as the warmer Atlantic surface water south of the PF causes sea-ice to melt. However, the sea-ice is an independent factor in controlling the position of the PF (Barton et al., 2018). A second local and seasonal feature, known as the "MW front" (of less than 50m deep) can often be distinguished from the PF during spring and summer, and it follows the ice edge northward as sea-ice retreats. Finally, a third nearby front can be found around the flank of Spitsbergen Bank around 50-100m depth, commonly referred to as the "tidal front." This front is formed through a horizontal density gradient resulting from strong tidal currents over a relatively shallow depth and has

also been associated with high biological production. It is particularly evident during the summer months but can be observed throughout the entire year (Fer & Drinkwater, 2014). The existence of three frontal systems in the area may each have different biological implications, which can make investigating their biophysical and ecological interactions complex.

The hydrographical frontal zone that coincides with the zoogeographical division creates ideal conditions for studying ecosystem dynamics along this gradient. Additionally, the Barents Sea is characterized by several biological hotspots, where physical processes drive and sustain biological activity, diversity, and productivity. Fronts have gained much attention in the biological and oceanographic community, as frontal processes have been found to play crucial roles on a global scale (e.g. thermohaline and gyre circulation) , as well as on a local scale (e.g. upwelling systems and partitioning of marine ecosystems) (e.g. Le Fèvre, 1987; Belkin et al., 2009; Belkin, 2021). For instance, fronts can create areas of high primary productivity due to vertical nutrient fluxes from enhanced mixing and upwelling, making them valuable for consumption by higher trophic levels (Le Fèvre, 1987; Martinetto et al., 2020). Fronts may also form regions of increased secondary production where zooplankton species aggregate (Franks, 1992). Aggregated organisms brought by the currents may therefore benefit from algal blooms along the PF while also serving as a potential food source for planktivorous fish.

Despite the PF being a dominant mesoscale feature in the Barents Sea with possibly high value to the entire ecosystem, there is currently limited knowledge about the role and importance of the PF to key planktivorous fish species and macrozooplankton (prey) distribution. Nevertheless, previous findings on enhanced primary production (Sakshaug et al., 1994) and secondary production (Basedow et al., 2014) in the PF area suggest that the PF may serve as an important foraging ground for pelagic fish like polar cod and capelin. It is generally understood that the habitat extent of marine ectotherms depends on various factors, including their temperature sensitivity (thermal tolerance), dispersal capacity (migratory vs. non-migratory), and the ability to exploit food resources (generalists vs. specialists) (Hoegh-Guldberg & Bruno, 2010; Sunday et al., 2012; Fossheim et al., 2015). Therefore, it is assumed that the thermohaline barrier imposed by the PF regulates the distribution of macrozooplankton (prey), which consequently influences foraging behaviour of planktivorous fish. Hence, the main objectives of this study are to: 1) examine how the hydrological features of the PF area influence macrozooplankton and fish distribution across the AW and ArW masses, and 2) to study the feeding behaviour (foraging activity and dietary structure) of capelin and polar cod across the PF. The interaction of the thermohaline and MW fronts is investigated. We used a combination of trawling mechanisms, broadband acoustics, and stomach content analysis to provide a direct reflection of species distribution and dietary structure in the PF area. While the overall scope of the project spans over three different seasons (spring, summer, and winter), this study highlights the spring season in late May 2022, a period of the highest primary production of the year.

2   MATERIALS & METHODS

2.1   Sampling area

*M*acrozooplankton and fish were collected in spring along a transect perpendicular to the PF (*Figure 6a*) onboard of the Helmer Hanssen. The ship left from Tromsø (Norway) on 2022-05-18 and returned on 2022-05-27. The transect went along (approximately) the 29° E longitude line through Hopen Trench, where a steep thermohaline gradient was expected to occur. Sampling was conducted over six Tucker trawl and five pelagic trawl stations (*Figure 6b*), with a sixth (northernmost) pelagic trawl station not being sampled due to ice conditions. Details on the sampling stations can be found in *Table 1*. The overall transect was split into two shorter transects, with the first transect consisting of stations PF2, PF4, and PF3, and the second of PF1, PF6, and PF5 (in chronological order). Ice cover initially prevented the vessel from going further north past PF4, but the conditions significantly improved as ice began to break up after PF1 (Appendix I, *Figure 19*). The northernmost station (PF6) was reached on 2022-05-24.

The hydrological regime in the study area is on the one hand influenced by the North-Atlantic current from the south that flows through Hopen Trench and splits into two branches: one leaving east in between Central Bank and Great Bank, and one leaving north where it descends underneath the ArW (and potentially returns along Spitsbergen Bank). On the other hand, the area is influenced by a south-westerly current of ArW origin that flows over Great Bank and Spitsbergen Bank. The depth profile of the transect went along the slope area of Hopen Trench; it was the deepest (max. ~ 375 m) at the most southern stations and became shallower as the vessel moved northward (min. ~ 200 m). A more precise location of the PF was obtained from regular measurements with the Seabird 911 Plus CTD profiler recording temperature, conductivity, and density of the water, from which temperature and salinity profiles could be derived.

Table 1: *details on the sampling stations.*

Trawl	Station	Date (yyyy-mm-dd)	Time (UTC+2)	Latitude (°)	Longitude (°)	Trawling depth (m)	Water T (C°)
Tucker	PF1	2022-05-23	09:48	74.97	29.09	75	2.8
			10:11			140	2.9
			10:42			250	2.7
	PF2	2022-05-20	00:28	75.01	29.60	140	3.2
			00:58			250	2.8
	PF3	2022-05-22	12:18	75.46	29.78	60	0.3
			12:35			120	0.6
	PF4	2022-05-21	16:45	76.05	29.34	115	-0.2
			17:22			230	-0.7
	PF5	2022-05-25	10:42	77.03	29.58	180	-1.5
	PF6	2022-05-24	23:35	77.54	29.99	25	-1.5
Pelagic	PF1	2022-05-23	06:47	74.98	29.01	70 & 140	3.0
	PF2	2022-05-20	07:23	75.01	29.57	55 & 140	3.2
	PF3	2022-05-22	07:09	75.49	29.56	60 & 100	0.1
	PF4	2022-05-21	20:31	75.98	29.52	118 & 200	-0.3
	PF5	2022-05-25	15:16	76.99	29.76	190	-1.5
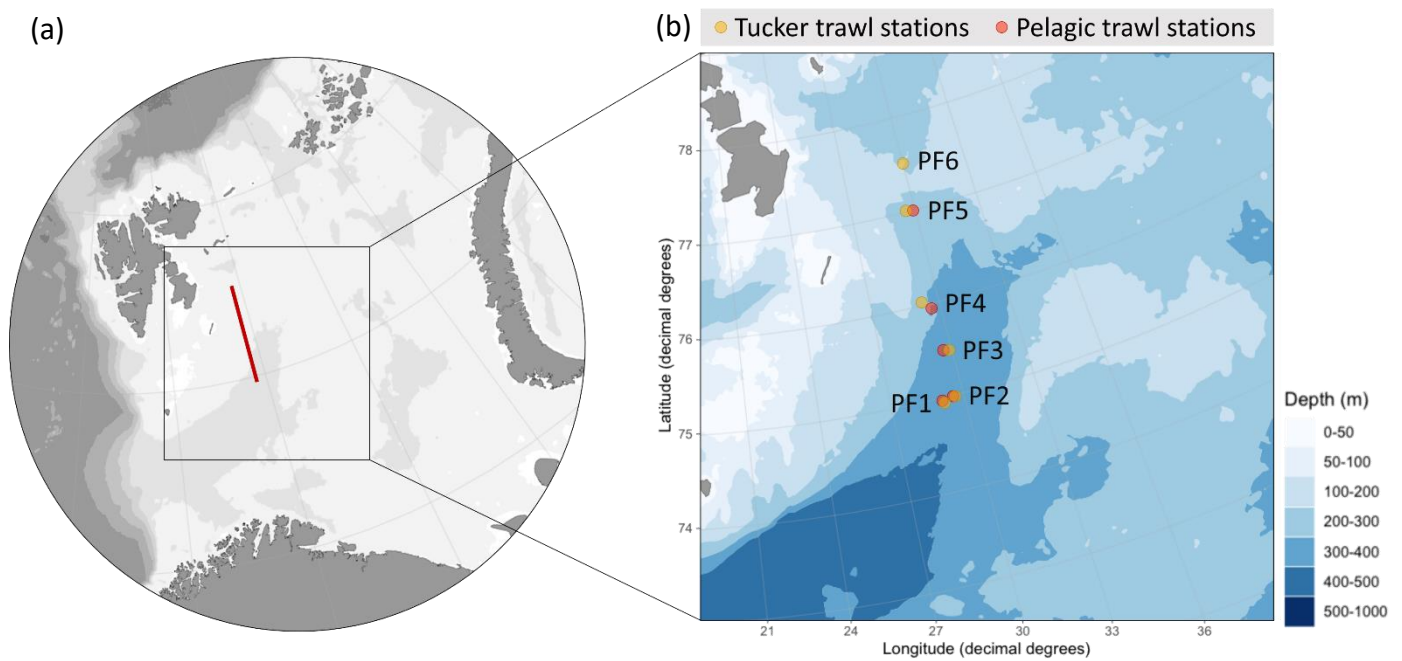
Figure 6: *map of **(a)** the transect location and **(b)** individual sampling stations for the Tucker and pelagic trawls.*

2.2   Sampling methods

Hull-mounted EK60

$\mathscr{B}$roadband acoustics were used to detect and locate organisms in the water column across the PF. The keel-mounted Simrad EK60 split-beam echosounder continuously recorded hydroacoustic data at 18, 38, and 120 kHz. The ping rate was set to 1.5 seconds and pulse length to 1,024 µs.

Tucker Trawl

Macrozooplankton were sampled with a Tucker trawl (*Figure 7a*) (1 m^2 opening and 1500 µm mesh size) and towed for 10 minutes at approximately 2 knots. The targeted depth at each station was determined from the sound scattering layer identified in the echogram from the vessel's echosounder. Relative abundance from the Tucker trawl samples were analysed per station, and each taxon was counted and dried at 60 C° in pre-weighted recipients for dry weight measurements. The obtained abundances were standardized and converted to catch per unit effort (CPUE), expressed in grams per minute. Photos of the catch overview can be found in *Figure 20* (Appendix II).

Harstad Pelagic Trawl

The Harstad pelagic trawl (*Figure 7b*) was deployed within the main sound scattering layer(s) to ground-truth the acoustic signal and sample fish for stomach contents, lipid analyses and stable isotopes. The pelagic trawl has an effective height of 9-11 m and width of 10-12 m when towed at 3 knots. The mesh size of the inner liner of the cod end was 10 mm. The pelagic trawl was towed at ca. 3 knots for 20-30 min and abundances were standardized by converting to CPUE (expressed in kilograms per minute). All organisms were identified to the nearest species or genus onboard (*Figure 8a,c*). Throughout all stations, capelin had a large size distribution (*Figure 8b*), so individuals similar in length were sorted into size classes (small (S), medium (M), and large (L)). The total number and weight of each species was recorded, and for large catches, subsamples of 20-30 individuals from each size class were taken for further analysis. An overview of the size distribution of the subsamples can be found in *Table 2*.
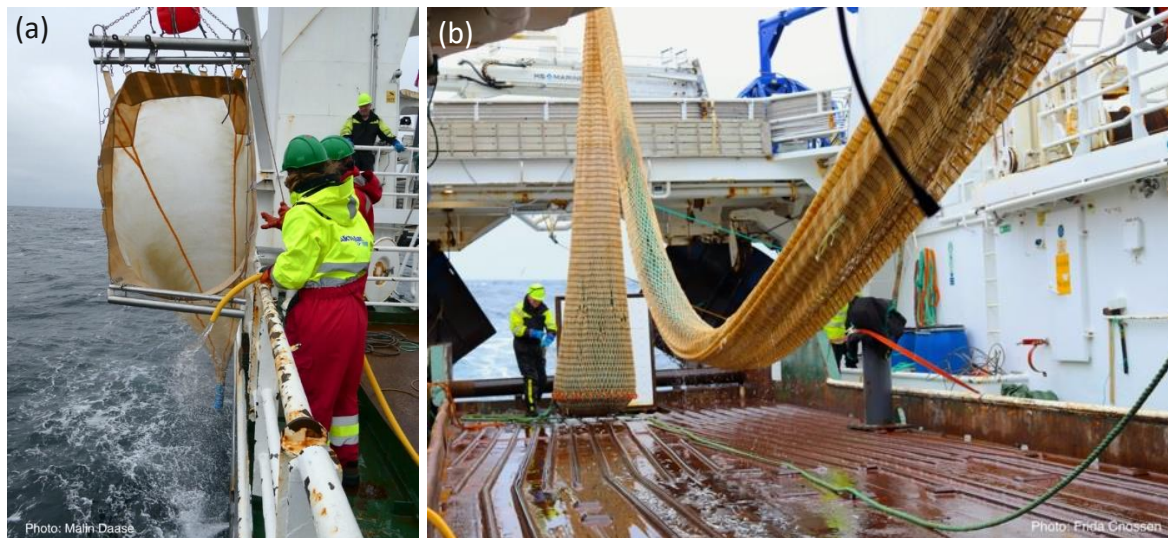
Figure 7: *deployment of **(a)** the Tucker trawl, and **(b)** the Harstad pelagic trawl.*

Stomach Contents

Data on fish diets were obtained through stomach content analysis from fish collected with the pelagic trawl. The standard length, height at the anus (to the nearest 1mm), and weight (to the nearest 0.1g) were measured for all specimens in the subsample. Afterwards, the stomachs were isolated (*Figure 8d*) and immediately preserved into 70% ethanol, and further analysis on the contents was conducted by trained and experienced personnel by use of a stereomicroscope (*Figure 8e*). While the stomach content analysis only provides a snapshot of the diet, the longer-term diet can be assessed through stable nitrogen isotope composition. This is a biomarker that is integrated in the muscle tissue over the course of weeks or months (Søreide et al., 2006). The dissected fish were preserved at -20 C for further analysis in the laboratory on land, but the results are excluded from this report.

For each individual stomach, a systematic visual assessment on the contents was applied. To get an indication on feeding intensity, the level of fullness was measured based on a quartile-scale (from 0 (0%): empty, to 4 (100%): full). To investigate prey composition qualitatively, the prey items were identified under a stereomicroscope to the nearest genus or species taxon. For the quantitative assessment, the count of each prey item (numerical method), the percentage volume each prey item takes up in the stomach (relative-fullness method), and the level of digestion for each prey item (from 1: newly eaten, to 5: digested or non-identifiable) (*Figure 8f*) were estimated and recorded. The combined numerical and volumetric approach of a was applied to reduce bias on the different prey items that could be found, while allowing for a quick and robust dietary overview. A more detailed discussion of methodologies for stomach content analyses is presented in Appendix I, *Table 4*.

Figure 8: ***(a)*** *sorting the pelagic trawl catch;* ***(b)*** *length distribution of capelin at PF1;* ***(c)*** *capelin (top), polar cod (middle) and redfish (bottom) caught at PF4;* ***(d)*** *dissecting the stomach of polar cod;* ***(e)*** *analysis of stomach contents under a microscope onboard; and* ***(f)*** *approximate five states of digestion of a euphausiid sp. used in assessing stomach contents.*

2.3   Analytical measurements on macrozooplankton

*T*o better understand the relationship between the zooplankton, sampling stations at various depths, and other (environmental) variables, a correspondence analysis was performed. The multivariate compositional data (by dry weight) of macrozooplankton from Tucker trawl samples from the different sampling stations comprised the primary data set as active points, whereas other factors of interest (temperature, depth, latitude, and richness) were added as supplementary points to discover features in the primary data. The dataset was standardized (mean equals zero) using the decostand function from the "vegan" package in R studio (Oksanen et al., 2022), and the "ca" package (Nenadic & Greenacre, 2007) was used to display the results in a biplot. The Euclidean distance was calculated to assess similarity among sampling sites and expressed as clusters in the biplot.

Additionally, differences in richness and species composition of zooplankton dry weight samples across sampling stations were analysed through beta diversity measurements, but the findings are excluded from the main results (mainly because of an uneven distribution among sampling sites in the AW and ArW). However, a more detailed description on this methodology can be found in Appendix I under "*Measuring beta diversity,*" and results shown in Appendix II (*Figure 22*) are briefly mentioned in the discussion section.

2.4   Analytical measurements on fish dietary structure

$\mathcal{T}$wo main objectives to be addressed during this study in assessing the fish dietary structure were 1) the foraging effort; 2) the relative diet composition. To get an indication on whether feeding was active, the foraging effort was estimated from calculating the average stomach fullness and total prey frequency. The average stomach fullness was obtained by adding the stomach fullness (between 0% (0) and 100% (4)) from each individual fish and dividing it by the total number of fish, multiplied by 100. The total prey frequency was calculated by adding the total number of ingested prey items per fish, and results were expressed in a boxplot. A non-parametric Kruskal-Wallis test was used to compare the total prey frequency values among fish size classes and sampling stations. To discern any significant differences (α = 0.05) between the fish groups, a non-parametric multiple comparisons Dunn-test was performed.

Stomach content analysis techniques in fishes are described by Sagar et al., (2019), from which equations were obtained and used as described below. An estimation of the relative diet composition was obtained from the volumetric data, as the size difference between the various prey species (e.g. one small copepod versus a 10 cm-long teleost) was considerably large, and thus would not give reliable results if solely expressed numerically. So, the percentage volume of each prey category ($\%V_i$) was obtained by calculating total volume for a particular prey item category (V_i), and dividing it by the total volume of prey items (V_t), multiplied by 100:

$$\%V_i = (V_i \,/\, V_t) \times 100 \tag{1}$$

To ascertain the overall importance of common food items to the fish diet, the Index of Relative Importance (IRI) was applied. This index makes use of a combination of the numerical and volumetric measurements as a more representative approach of the overall dietary composition. The percentage by number ($\%N_i$) was obtained in a similar way by calculating the total number of a particular prey item category (N_i), and dividing it by the total number of prey items (N_t), multiplied by 100:

$$\%N_i = (N_i \,/\, N_t) \times 100 \tag{2}$$

The IRI also considers the percentage frequency of occurrence ($\%O_i$; also known as the presence-absence method), which relies on the positive identification of prey items without taking its relative contribution into account. This can be obtained by adding the number of stomachs containing prey item i (O_i), and dividing it by the total number of stomachs containing food (O_t), multiplied by 100:

$$\%O_i = (O_i \, / \, O_t) \times 100 \tag{3}$$

Then, the IRI was calculated as followed:

$$IRI = (\%N_i + \%V_i) \times \%O_i \tag{4}$$

Where $\%N_i$ = the percentage of specific food categories by number;
$\%V_i$ = the percentage of specific food categories by volume; and
$\%O_i$ = the frequency occurrence

Finally, the non-parametric Mann-Whitney test was used to examine preferences for particular prey item categories among capelin size classes.

3   RESULTS

3.1   CTD and acoustic measurements

$\mathcal{T}$he Seabird 911 Plus CTD® enabled us to determine the hydrological characteristics of the different water masses occurring in the sampling area, as well as the approximate position of the PF (*Figure 9*). The AW ($T \sim$ >1.0 °C, S > 35.0 psu) occurred south of the PF at PF1 – PF5, and met with the ArW ($T \sim$ <0 °C, S < 34.8 psu) in the north where PF6 was sampled. Colder AW temperatures (1.0 – 3.0 °C) were found at PF3 – PF5, and stations PF1 and PF2 occurred in warmer AW temperatures (>3.0 °C), while salinity stayed constant. Additionally, a MW layer (T > 0.0 °C, S < 34.2) appeared in the upper ca. 40m of the water column at PF3 – PF5, with PF5 being directly south of the PF.
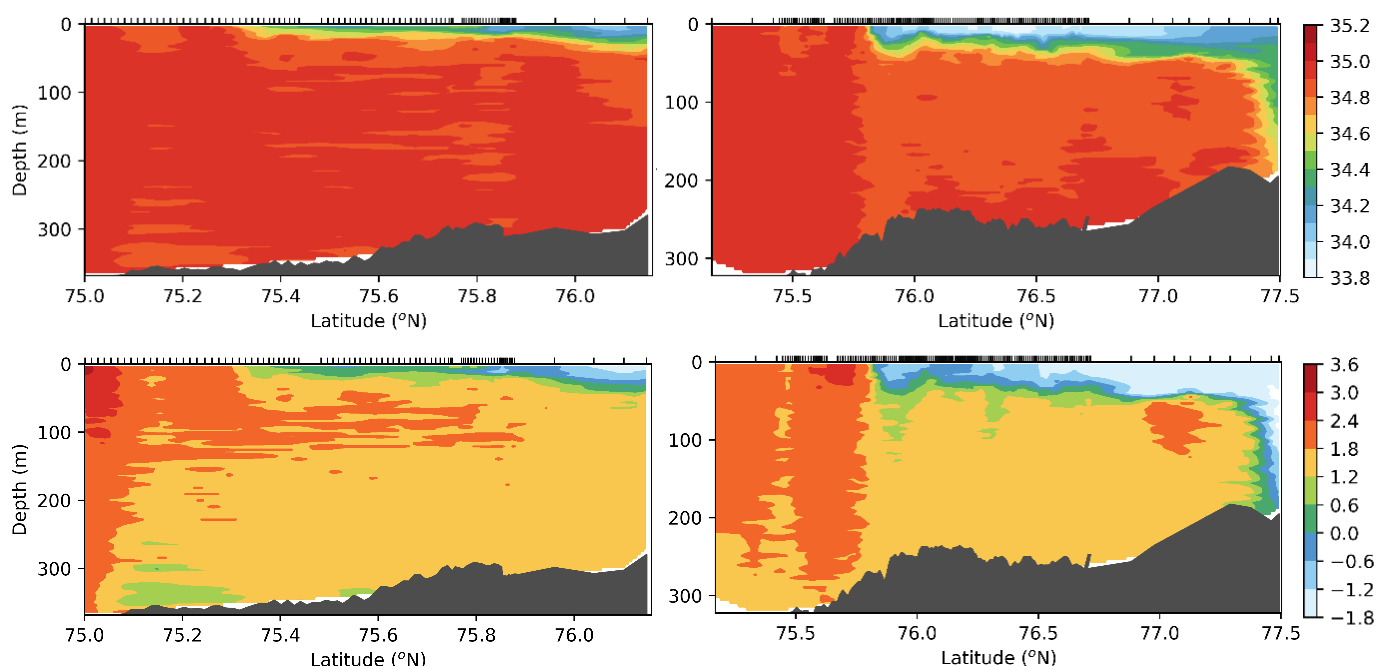
Figure 9: *Salinity (top) and temperature (bottom) profiles of the PF area. Left and right diagrams show the first (PF2 – PF4) and second (PF1, PF5, and PF6) transects, respectively. Preliminary data from S. Basedow.*

The vessel's EK60 split-beam echosounder data shows patches corresponding to differently sized organisms (*Figure 10*). The 120kHz data allowed for detection of a range of smaller organisms (e.g. macrozooplankton), while the 38 kHz and 18 kHz were suitable for detecting larger organisms (e.g. fish schools). Preliminary results show that most acoustic backscatter remained in the AW, with low backscatter in the ArW and MW. Concentrated backscatter near the bottom south of the PF can be seen from the 120 kHz profile, while moderate intensities appeared closer to the surface at PF6. The 38 kHz and 18 kHz profiles display patches of intense backscatter mostly throughout the water column, with a few smaller patches near the bottom. The overall backscatter of the 38 kHz and 18 kHz was lower north of the PF, and high intensities occurred further south of the PF. Strong acoustic signals also appeared to be closer to the surface, such as at PF2 (Appendix II, *Figure 21*).
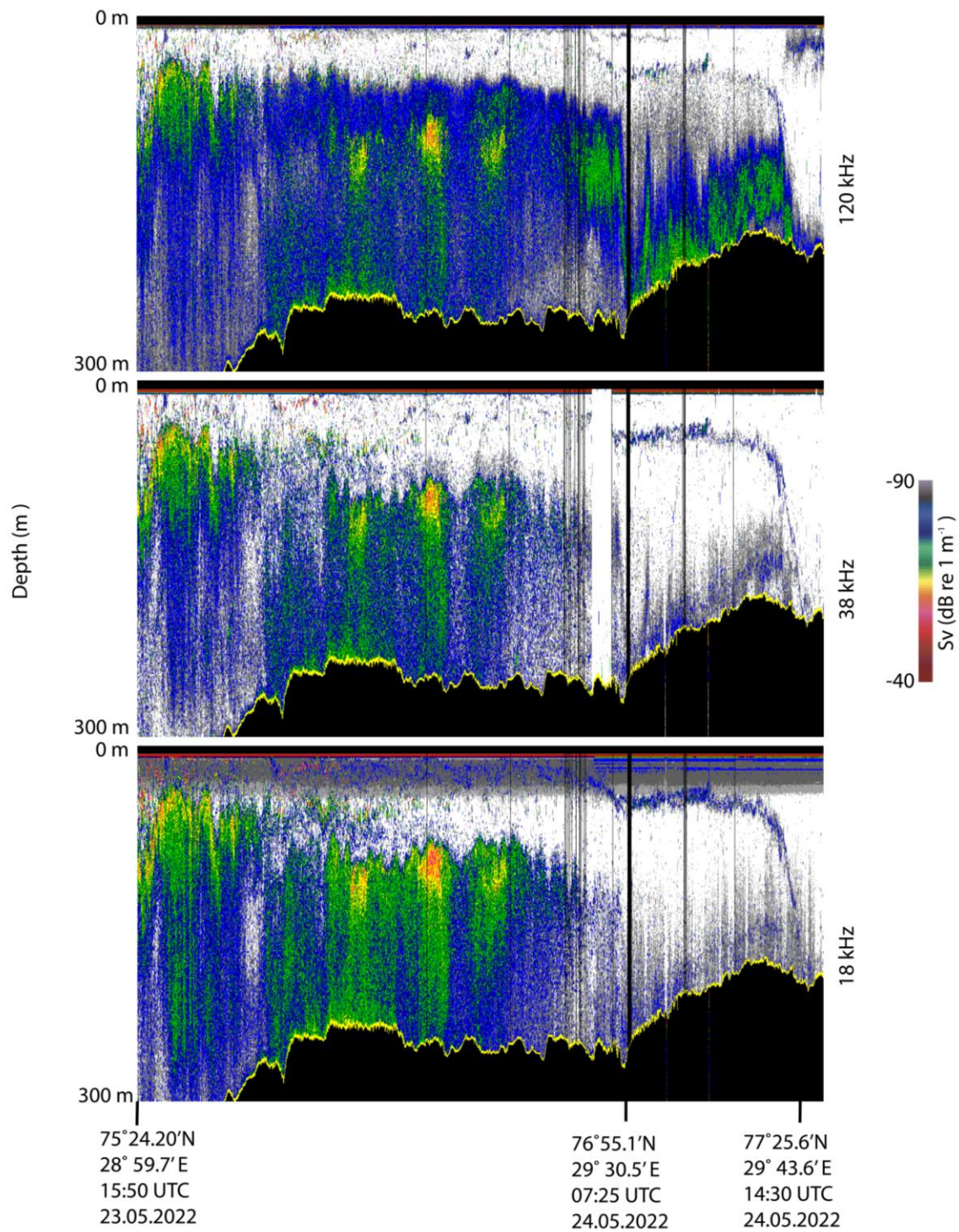
Figure 10*: EK60 echograms at frequencies of 120 kHz, 38 kHz, and 18 kHz at the northern side of the sampling area (PF5-PF6) near the PF. Preliminary data obtained from M. Geoffroy.*

3.2   Catch overview of the Tucker and Harstad pelagic Trawls

igure 11 shows the catch per unit effort (CPUE) for the macrozooplankton and fish composition from the Tucker Trawl and Harstad pelagic trawl, respectively. Macrozooplankton and fish appeared with large variations in biomass between the stations. The highest and lowest Tucker trawl catches were recorded at PF6 (6.49 g min^{-1}) and PF3 (0.16 g min^{-1}), respectively. For the pelagic trawl, the highest and lowest biomasses were obtained at PF1 (10.94 kg min^{-1}) and PF5 (6.00 kg min^{-1}), respectively. At stations PF2-PF4, where zooplankton abundance was relatively low, fish abundance was comparatively high, and *vice versa.*
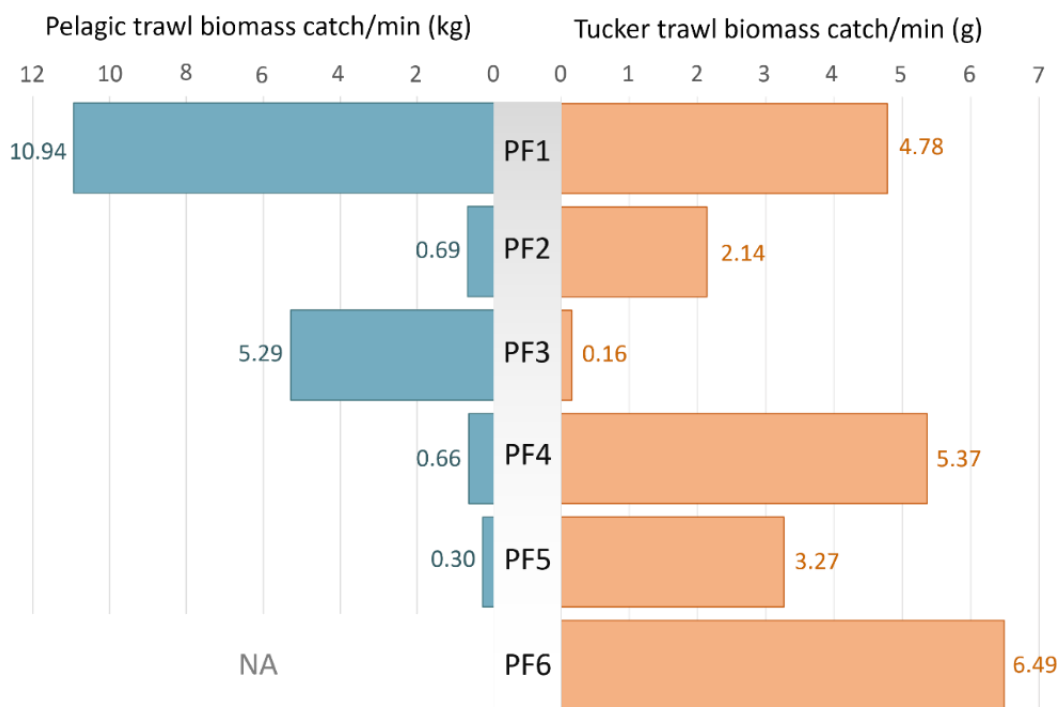
Figure 11: *Catch overview of the Harstad pelagic trawl (kg min^{-1}) (left) and Tucker trawl (g min^{-1}) (right) at each station. NA indicates no pelagic trawl was taken at PF6 due to ice conditions.*

Zooplankton community composition

The relative dry weight (*Figure 12*) and numerical macrozooplankton composition (*Figure 13*) (with copepods being excluded from the count due to very high numbers) were determined from the Tucker trawl samples. A total of 23 macrozooplankton species taxa were recorded, consisting of 20 and 12 different species in the AW and ArW, respectively (Appendix I, *Table 5*). The greatest richness (16) was found at PF4 and PF5. The catch at PF1-PF5 consisted mostly of euphausiids, chaetognaths, copepods, and some other forms of gelatinous zooplankton (cnidarians, ctenophores, siphonophores). Copepod species *C. finmarchicus, M. longa,* and to a lesser extend *C. hyperboreus* occurred in low abundances at

these stations, while *C. glacialis* and *C. hyperboreus* were abundant at PF6. At PF1, high mortalities of *Calanus* spp. (primarily *C. finmarchicus*) were observed, while other copepod species (*M. longa*) were found alive. The larger carnivorous copepod *P. norvegica* was found at PF1 and PF4 with blue ovisacs attached to the body. Euphausiids were caught across all stations, except for PF3 where the net was close to empty. Among the euphausiids, *T. inermis, T. longicaudata* and *M. norvegica* were observed in descending abundances. *M. norvegica* was found at PF1 and PF4, but was more frequently observed in the pelagic trawl net. Among the chaetognaths, *Eukrohnia hamata* was generally the dominating species, followed by *Parasagitta elegans*. Other gelatinous taxa from the phyla cnidaria (*Aglantha digitale* and *Euphysa flamea*), ctenophora (*Beroe cucumis*), siphonophora (indet.) and mollusca (order pteropoda: *Clione limacina* and *Limacina helicina*) were commonly caught in the nets as well. Samples from the two most northern stations also contained several amphipods, including three hyperiid amphipods (*T. libellula, T. abyssorum,* and *Hyperoche medusarum*), and one ice-associated amphipod *Apherusa glacialis*. Additionally, unidentified fish eggs were found at PF1-PF4, and two polar cod larvae were found at PF6. Other species sporadically observed and classified included decapod larvae (*Pandalus borealis, Sabinea sp.,* or unidentified), and Mysidacea sp.
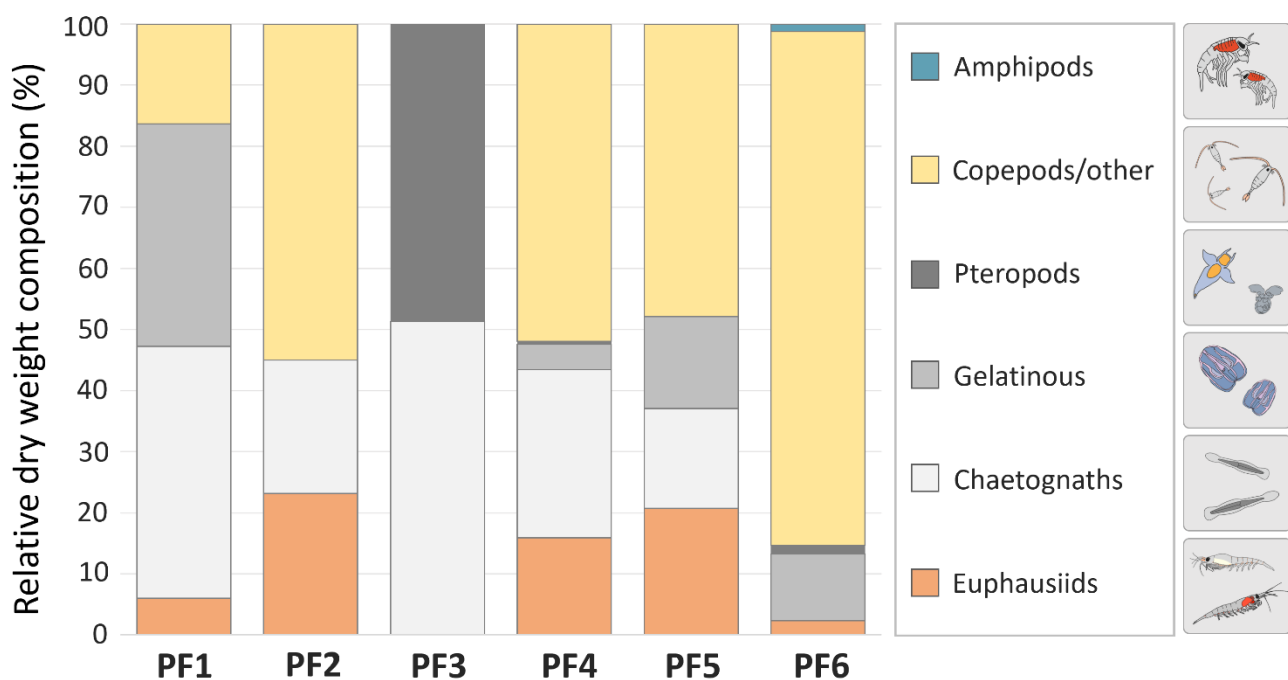
Figure 12*: Relative catch composition (% dry mass) of zooplankton sampled from the Tucker trawl.*
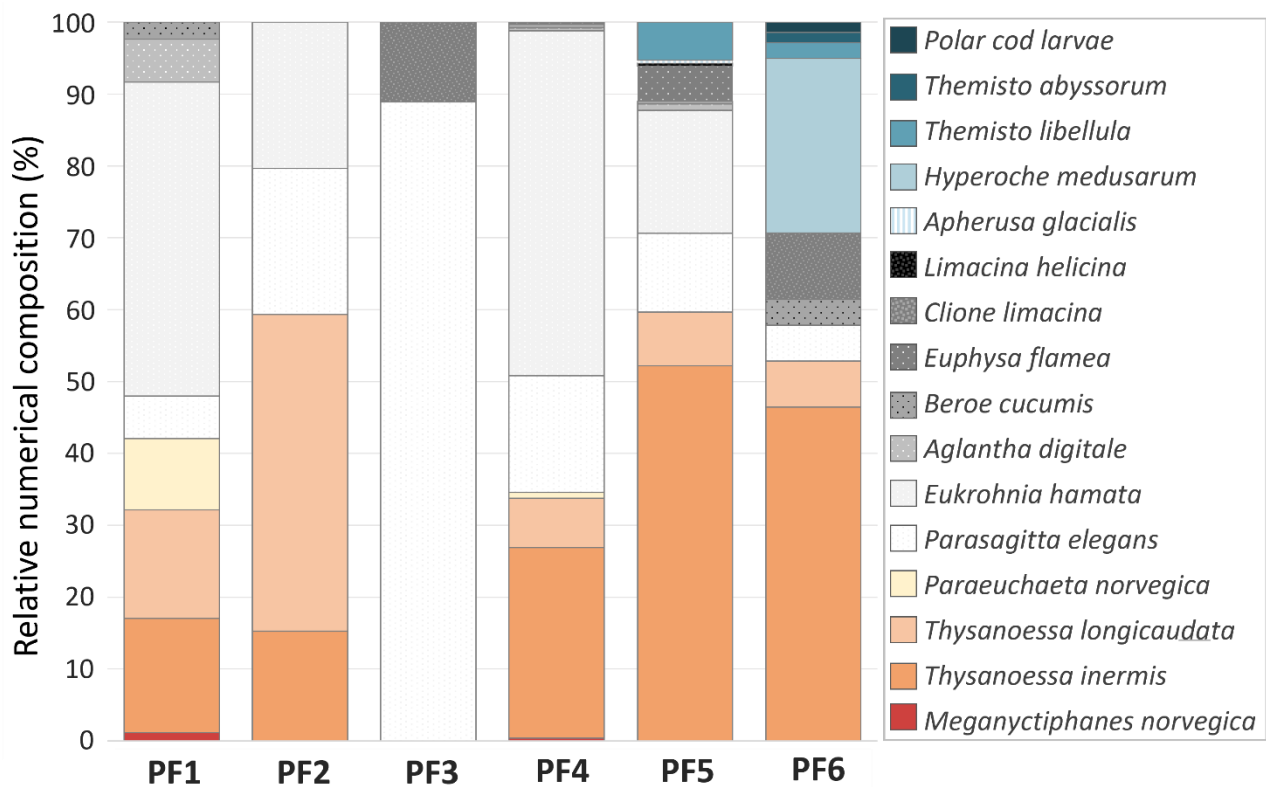
Figure 13*: Relative catch composition (% individuals) of zooplankton sampled from the Tucker trawl.*

The correspondence analysis explains a total of 88.4% of the observed variation (*Figure 14*). Two distinctive clusters could be determined and largely separated deeper from shallower stations. Exceptions to these clusters were the deepest most Atlantic station (PF1, ~250m depth) and the shallowest Arctic station (PF6, ~25m depth). The stations PF1-PF3 were less discriminating, which corresponds to the relatively empty catches taken from these depths. The analysis shows that euphausiids and chaetognaths were mostly associated with greater depths in the AW, and other gelatinous zooplankton demonstrated a strong relationship with temperature. The richness was largely determined by the presence of euphausiids in the samples and was the greatest at the deeper stations south of the PF. Copepods were mostly associated with higher latitudes, though its position in the diagram is the least discriminative compared to other organisms. Finally, pteropods and amphipods were mostly associated with the shallow Arctic station PF6.
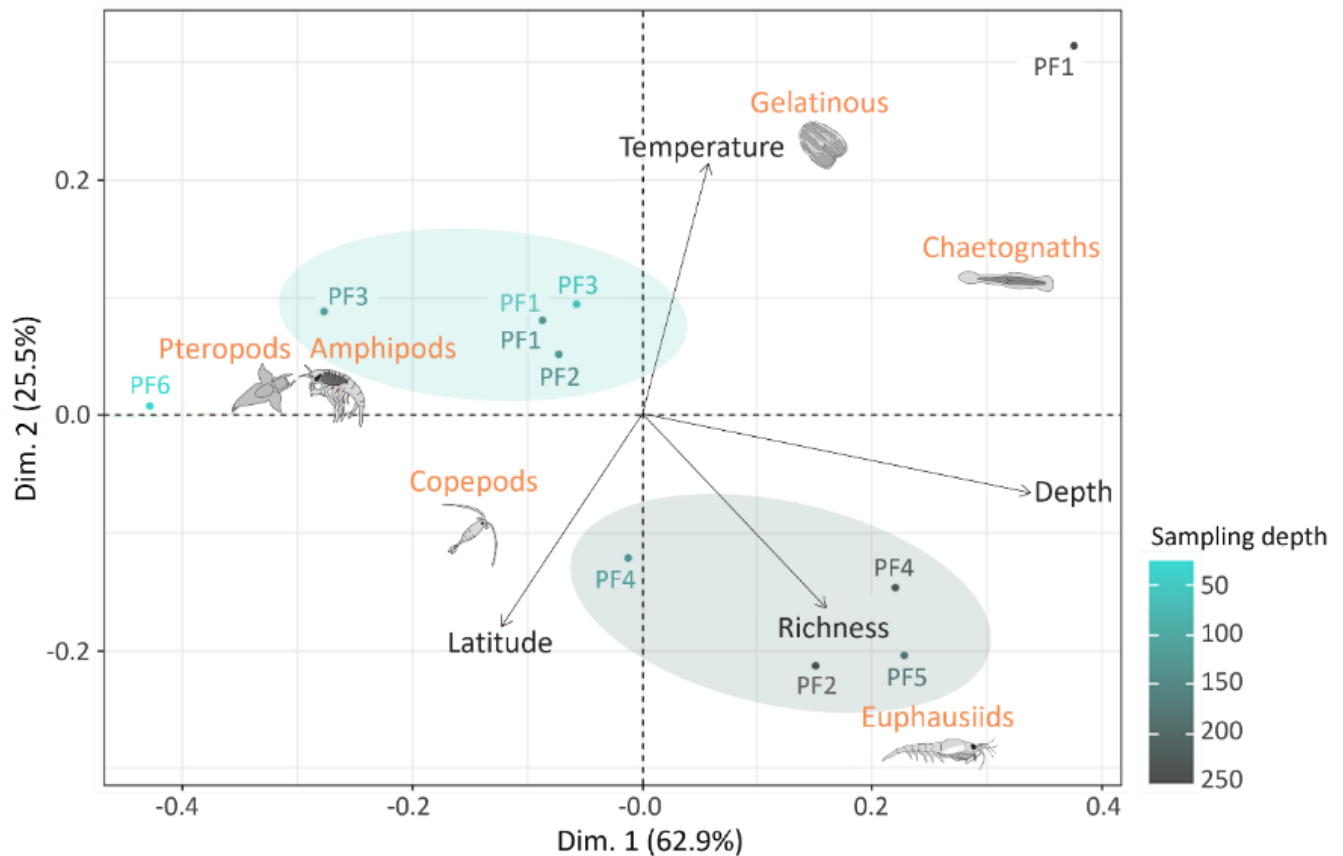
Figure 14: *Correspondence analysis biplot showing the association among zooplankton composition (based on dry mass) per Tucker trawl sample. Depth of the sample is indicated by the colour of the sample label. Centres of mass for the main plankton groups are indicated by the pictograms. Environmental factors (temperature, latitude, depth) and total taxonomic richness were added as supplementary variables and are indicated by vectors. Clusters were determined by Euclidean distance-based similarity and are indicated by ellipses.*

Fish community composition

The relative catch composition in biomass from the pelagic trawl is shown in *Figure 15.* Capelin was caught at all stations (PF1-PF5) and consisted of predominantly medium-sized fish (7.6 – 12.7 cm), with a lesser proportion of smaller (6.8 – 9.5 cm) and larger (11.0 – 14.6 cm) individuals (*Table 2*). Polar cod was caught at the three most northern stations at temperatures ranging from 0.29 °C to -1.46 °C, and with a length distribution of 9.0 – 19.0 cm. Additionally, a few other species were caught, including some small redfish (*Sebastes sp.*) at PF4, and one small haddock (*M. aeglefinus*) at PF5. Frequently the catch also included euphausiids, especially at PF5, and except for PF1 where the catch consisted solely of capelin. The trawl mesh size does not retain all euphausiids, so the absolute catch biomass of euphausiids is not included in *Figure 15*. Other species observed were the shrimp *P. borealis* at PF4, as well as the cnidarian *Ptychogena lactea* at PF5.
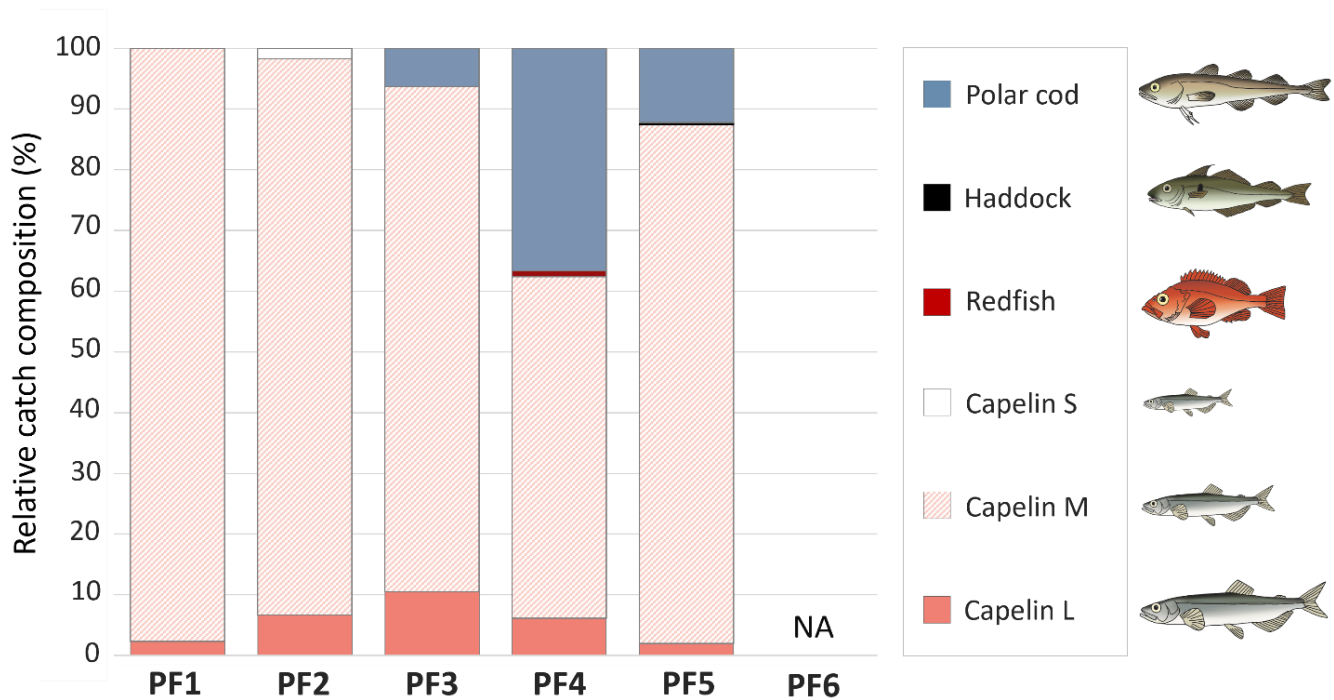
Figure 15: *Relative catch composition (% wet mass) of the Harstad pelagic trawl per station. NA: no data available.*

3.3   Stomach content analysis

tomach contents from a total of 90 polar cod and 250 capelin were analysed, with the latter separated by size - 30 small, 110 medium, and 110 large individuals. Percentage empty stomachs (*Table 2*) and stomach fullness (*Figure 16*) were derived from the stomach content data. Capelin collected from the pelagic trawl showed high percentages of empty stomachs (60 – 93%) and low stomach fullness (0.16 – 8.25%) at stations PF1-PF4. However, only one empty capelin stomach was found at PF5, and the stomach fullnesses here were 39.0% and 64.1% for medium and large-sized fish, respectively. In all cases, small to medium-sized capelin had higher percentages of empty stomachs than large sized capelin. On the contrary, polar cod were feeding across all stations they were caught (stomach fullness 31.7 - 43.3%), and no empty stomachs were observed. The highest stomach fullness of polar cod was found at PF5 (43.3%).

Table 2: Number of fish analysed with corresponding size distribution and percentage empty stomachs per station

Station	Fish species	N	Size class	Length (cm)	% Empty stomachs
PF1	Capelin	20	M	8.0 - 10.5	90
		20	L	11.0 - 14.0	80
PF2	Capelin	30	S	6.8 - 9.5	93
		30	M	8.3 - 12.5	63
		30	L	11.8 - 14.4	60
PF3	Capelin	20	M	9.5 - 12.7	85
		20	L	11.7 - 14.6	80
	Polar cod	30	-	9.3 - 12.7	0
PF4	Capelin	20	M	7.6 - 10.5	90
		20	L	11.5 - 14.5	85
	Polar cod	30	-	10.0 - 19.0	0
PF5	Capelin	20	M	9.5 - 12.0	5
		20	L	12.0 - 14.5	0
	Polar cod	30	-	9.0 - 16.5	0

The volumetric prey composition (*Figure 16*) and %IRI values (*Table 3*) highlight the relative prey importance to the dietary structure of capelin and polar cod across the PF. The main prey items contributing to the bulk of the stomach contents for both fish were euphausiids (capelin 16.5 – 76.6 %IRI; polar cod 62.0 – 96.4 %IRI) and copepods (capelin 0 - 54.0 %IRI; polar cod 0.46 - 37.6 %IRI), as well as some teleosts for polar cod. Copepods were numerically more common in the diet of medium-sized capelin of lengths <12.0 cm (Mann-Whitney test, W = 40, *p* = 2.1e-4), whereas euphausiids were eaten more frequently by larger individuals of lengths >12.0 cm (Mann-Whitney test, W = 258.5, *p* = 8.5e-5). The same was also seen to a lesser extent for polar cod, as larger prey items including teleosts (mostly capelin of lengths $\sim 9.0 - 11.0$ cm) were only observed in larger-sized polar cod at PF4 (length $13.0 - 17.5$ cm) and PF5 (length $15.5 - 16.5$ cm). Amongst euphausiids that could be differentiated, *T. inermis* was generally the dominating species, and *T. longicaudata* and *M. norvegica* occurred seldomly. The copepods were often too digested to be reliably distinguished to species taxon. Other prey items sporadically found in the stomachs included a decapod, a fragment of *P. borealis,* the hyperiid amphipod *H. medusarum*, and *P. norvegica.*
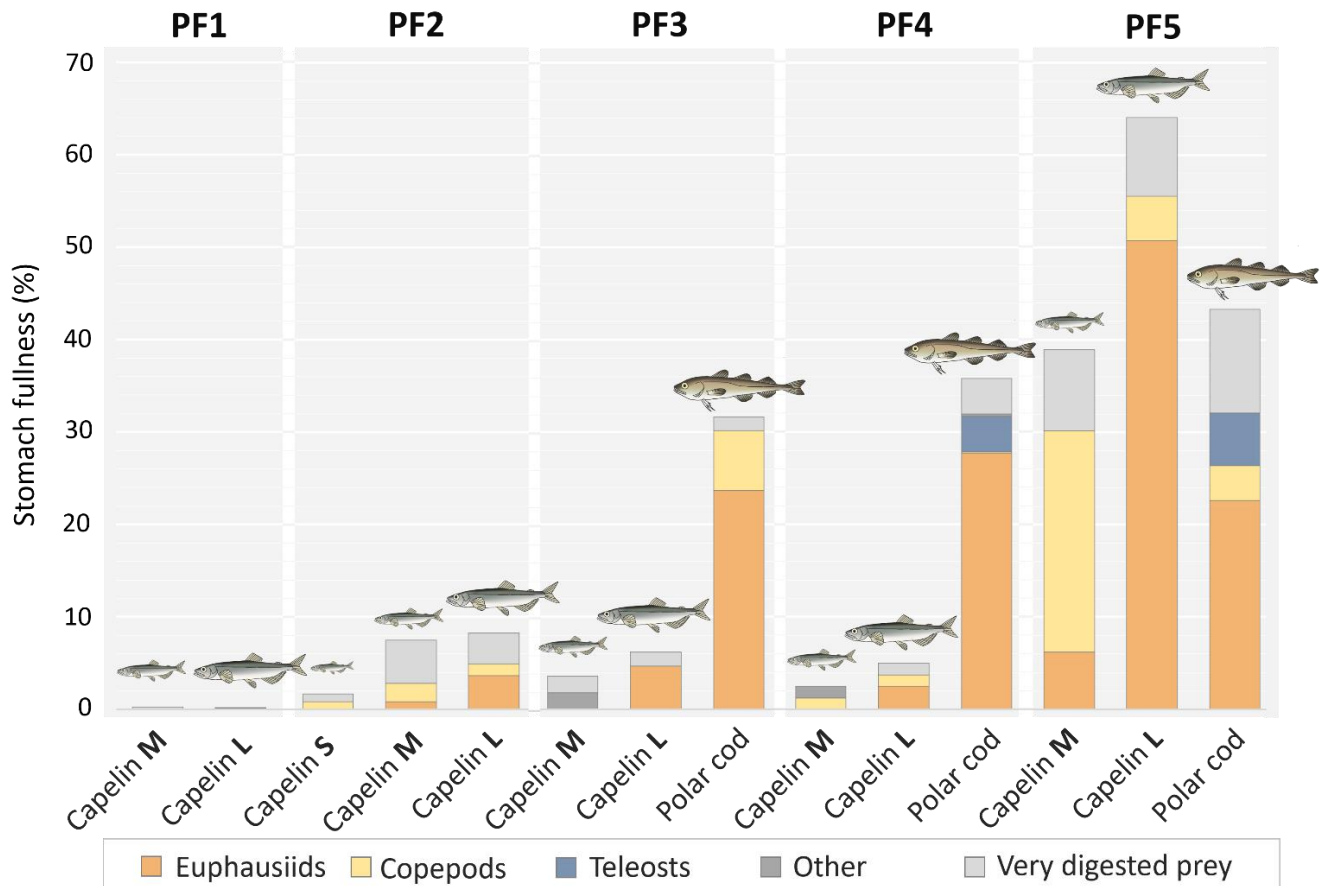
Figure 16: *Prey composition and percentage stomach fullness of fish sampled with the Harstad pelagic trawl across the stations.*

Table 3: *Index of Relative Importance (%) for capelin (top) and polar cod (bottom).*

%IRI Capelin

Prey item	PF1*	PF2*	PF3*	PF4*	PF5
Euphausiidae	76.6	16.5	73.5	40.0	43.0
Copepods	6.20	25.8	0.00	40.0	54.0
Teleosts	0.00	0.00	0.00	0.00	0.00
Other	0.00	0.00	5.31	10.0	0.00
Unidentified	17.3	57.7	21.2	10.0	3.01

*Based on limited data due to high percentage of empty stomachs

%IRI Polar cod

Prey item	PF3	PF4	PF5
Euphausiidae	62.0	96.4	70.8
Copepods	37.6	0.46	12.1
Teleosts	0.00	1.49	2.71
Other	0.00	0.63	0.00
Unidentified	0.46	0.99	14.5

The foraging effort expressed in total prey frequency (*Figure 17*) shows a similar trend to the stomach fullness described above, with high feeding activity near the PF. The boxplot shows significant differences between the median values (Kruskal-Wallis test, H = 227.29, df = 13, p < 2.2e-16). Post-hoc analysis revealed two significantly different groups, indicated by the letters *a* and *b* (Dunn-test, p < 0.05). The foraging effort of capelin at PF5 (median 4 – 6) was significantly higher than for capelin at all other stations (median 0 – 1), and the feeding activity of polar cod (median 2 – 4) was significantly higher than capelin at stations PF1-PF4. Group *b* showed a large range in feeding activity for both capelin (0 – 21 prey) and polar cod (1 – 17 prey) compared to group *a* (max. 3 prey). Amongst polar cod, no significant differences in feeding activity could be found.
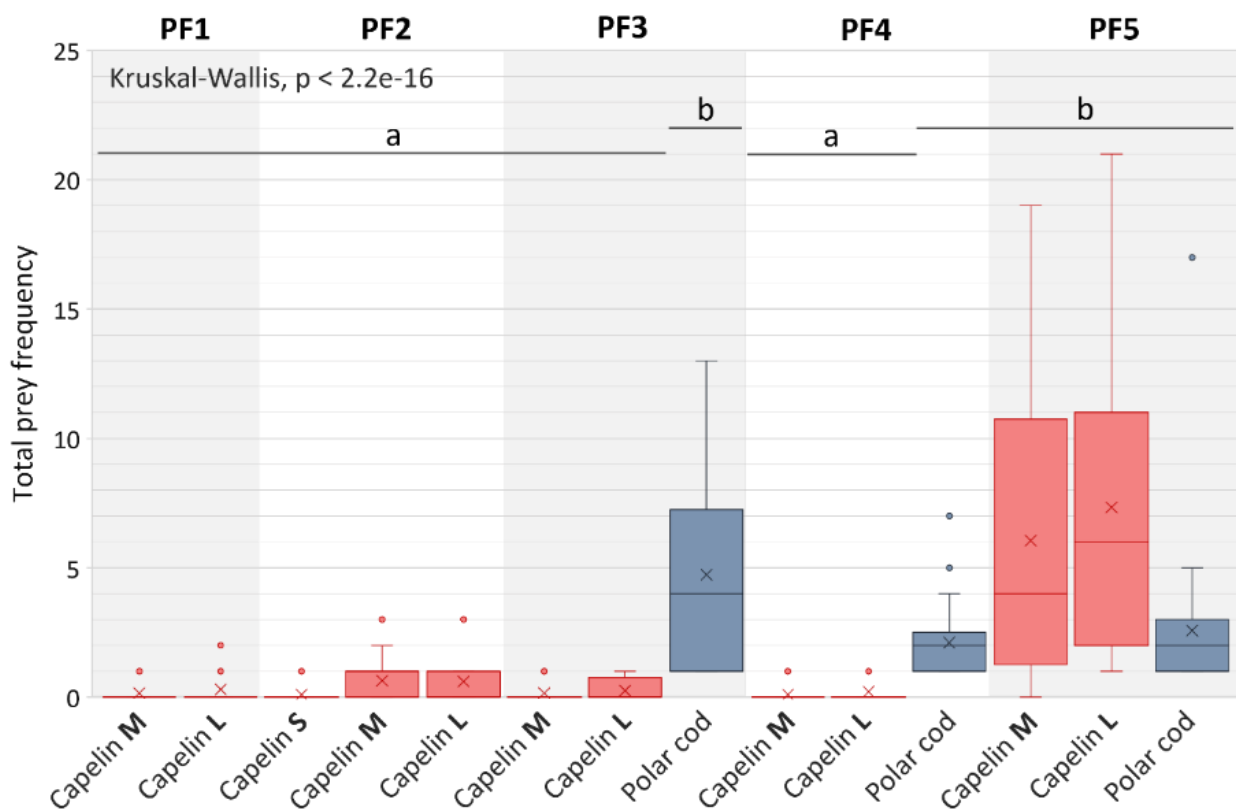
Figure 17: *Boxplot of foraging effort expressed as total prey frequency per fish across the stations. Means are indicated with x, and significant differences (Kruskal-Wallis, p < 2.2e-16) were found among the medians (lines in the boxplot). Significantly different groups (Dunn-test, p < 0.05) are indicated with letters* a *and* b *above the boxplots. Outliers (dots) were included in the tests.*

4   DISCUSSION

*T*he Barents Sea PF is an area of high importance to the biological system, and the ecosystem dynamics surrounding the PF need to be properly understood to sustain its ecological integrity. It is a feature of high ecological value to a wide spectrum of organisms, yet sensitive to the impact of human activities and environmental changes. With the lack of knowledge on how the PF regulates the macrozooplankton (prey) distribution across the AW and ArW masses and how this could be significant to planktivorous fish, there was a need to acquire an in-depth understanding on the biophysical structure of this region. It was assumed that the thermohaline barrier imposed by the PF acts as a distributional boundary in regulating zooplankton prey, which consequently influences the feeding behaviour of fish. Therefore, as part of the overall POLARFRONT project, this study reports on the distribution, composition, and food-web dynamics of macrozooplankton communities and pelagic fish at the PF in late May 2022. In combination with the current understanding from previous studies, the results showed that the PF acts as a distributional boundary among macrozooplankton groups, and diets of key pelagic fish species varied over a relatively short spatial scale, with planktivorous fish taking advantage of PF-related prey aggregations.

4.1   Biophysical structure of the Polar Front area and macrozooplankton distribution

*T*he CTD showed a steep thermohaline gradient at the transition between the AW and ArW masses, and a coincident pattern in acoustic backscatter was visible when matched up with the vessel's EK60 data. However, some of our observations on the macrozooplankton structure near the PF were also partially controlled by other local co-occurring oceanographic features. This includes a MW front induced by melting sea-ice, which is partly responsible for phytoplankton bloom formations (Daase et al., 2021). In fact, a previous study on the macrozooplankton communities across the water masses found that ice cover and algal blooms were not linked with the horizontal macrozooplankton distribution in May (Søreide et al., 2003). This suggests that the MW front was likely an independent factor with distinct effects on the local macrozooplankton structure in our study. For example, backscatter data indicated an avoidance of the MW layer (0-30 m) by both macrozooplankton and fish. Therefore, the observed biological interactions associated with the PF area in this study should be viewed as a result of the combination of two main events, namely 1) the thermohaline barrier imposed by the frontal boundary between AW and ArW masses, and 2) the MW front that roughly coincided with the location of the PF in spring.

The thermohaline barrier (Polar Front)

Comparison of the CTD profiles with the EK60 data and Tucker trawl samples showed that the thermohaline features of the PF created clear segregation of organisms between the AW and ArW masses. Most biological backscatter was seen in the deeper AW, with very low

backscatter in the ArW and MW, except for some in the ArW surface layer (see *Figure 10*). Tucker trawl results confirmed the presence of euphausiids and chaetognaths dominating the AW samples, and copepods were the primary organisms in the ArW sample (*Figure 18*). In contrast to other existing oceanic fronts, the PF is considered to be primarily a passive front, with circulation patterns not being strong enough to continuously supply nutrients to the euphotic layers (Drinkwater & Tande, 2014). However, it plays a major role in differentiating community structures, and has previously been observed to maintain fairly distinctive communities on both sides (e.g. Søreide et al., 2003). The Atlantic side has generally been described as more productive during sampling in August (Basedow et al., 2014) and is characterized by more abundant planktonic communities with greater diversity (Trudnowska et al., 2016; Mańko et al., 2022). In fact, the greatest diversity of macrozooplankton taxa (16) was observed in the AW at PF4 and PF5. The steep biological gradient found in our study adds to the large body of literature that advocates that water mass distribution is a key determinant in structuring planktonic communities.

Additionally, the 120kHz backscatter showed macrozooplankton accumulations closest south of the PF. Hydrographic patchiness from small-scale variability in physical conditions at the PF has been shown to mirror a patchy zooplankton distribution (Våge et al., 2014). However, previously investigated zooplankton patchiness at the PF appeared in various sizes (5 – 50m), where small-scale hydrological features were closely related to patches of small-sized fractions (i.e. phytoplankton, marine snow), while biological factors were thought to have a greater influence on patches with larger-sized organisms (i.e. *Calanus* spp.) (Trudnowska et al., 2016). Therefore, it is likely that both hydrographical conditions and biological facets have contributed to accumulation events in our study, depending on the size and nature or phenology of the species.

The meltwater front
The MW front impacted primary and secondary productivity in the area, which eventually influenced macrozooplankton abundances and diets of capelin and polar cod. The MW layer was induced by ice cover that extended south of the PF in the AW and led to a(n) (early) stratification of the water column upon melting. In fact, colleagues identified high chlorophyll *a* biomass at PF3 and PF4 in the uppermost ca. 20-25m of the water column within the MW layer. On the contrary, phytoplankton sampled at PF1 and PF2 occurred in the well-mixed layers of the water column at 80-100m, and the near-surface bloom at PF5 and PF6 had not reached its peak yet (E. Leu, unpublished data). Copepods, including *Calanus* spp. that dominate the biomass in the Barents Sea and all Arctic systems and (Daase et al., 2021), were found in low abundances across all AW stations (PF1 – PF5). CV stages and females dominated across most AW stations (M. Daase, unpublished data) and these are associated with overwintering stages (Daase et al., 2021). Only in the upper layer of the ArW (PF6) were *Calanus* spp. observed in moderate densities, implying feeding activity. Thermocline formation, which triggers the phytoplankton bloom in the AW (Daase et al., 2021), had not been clearly established yet at the southernmost stations (PF1 and PF2), and the deeper well-

mixed phytoplankton coincided with the absence of zooplankton blooms. The high occurrence of carcasses of *Calanus* spp. sampled at PF1 may have been the result of non-consumptive mortality, a phenomenon observed earlier among *Calanus* spp. in the Arctic Ocean during winter. In this case, other stressors (e.g. deficiency of essential substances, environmental conditions) may have been responsible for the observed mortality, rather than of predation (Daase et al., 2014). At PF3 and PF4, the early occurrence of intense phytoplankton blooms showed a mismatch in time with and planktonic grazers. Nonetheless, fluctuations in the timing of sea-ice break up create a certain level of unpredictability for the biological activity in the area (Lien, 2018), and enhanced primary productivity at the PF can only be observed in some years (Reigstad et al., 2011). A mismatch resulting from an early stratification induced by sea-ice passing into the AW is not uncommon (Vinje, 2009), but can have negative consequences for grazers and other organisms depending on this (Søreide et al., 2010).

Macrozooplankton composition in the Atlantic Water

Tucker trawl samples from stations in the AW consisted mostly of organisms related to subarctic and boreal regions (Appendix II, *Table 5*) and were dominated by euphausiids (*T. inermis, T. longicaudata,* and *M. norvegica*), chaetognaths (*E. hamata* and *P. elegans*) and copepods (mostly *C. finmarchicus, M. longa,* and *P. norvegica*), as well as the frequent occurrence of cnidarians (*A. digitale* and *E. flamea*), ctenophores (*B. cucumis*), and pteropods (*C. limacina*). The presence of *T. longicaudata* and *M. norvegica* is a good indicator of AW, as these spawn in the Norwegian Sea and drift into the Barents Sea with the currents (Eiane & Tande, 2009), and are more abundant during warm years (Zhukova et al., 2009; Orlova et al., 2013). *T. inermis* also relies on advected populations from the Norwegian Sea, but has reproducing populations in the Barents Sea as well (Zhukova et al., 2009). It is usually the dominating species in regions with AW (Orlova et al., 2015), and its abundance in ArW is usually considerably lower (Dalpadado & Skjoldal, 1996). Gelatinous zooplankton have been found to be largely structured by water mass temperatures across the Arctic and Polar Fronts in the European Arctic (Mańko et al., 2022), and showed a strong association with temperature in the correspondence analysis. In fact, *A. digitale* was only observed in the AW, and has been said to be a good indicator on the Atlantic side of the PF (Mańko et al., 2022). Overall, the macrozooplankton community composition as described here was closely related with the hydrographical conditions of the AW.

AW samples contained a greater proportion of omnivorous (*T. longicaudata, M. norvegica, M. longa*) and carnivorous species (*P. norvegica,* chaetognaths and other gelatinous zooplankton) compared to ArW samples (Appendix II, *Table 5*). Omnivorous species are less subject to seasonal food shortages related to timing of algal blooms (Hagen, 1999), and the distribution and life histories of carnivorous zooplankton are tightly linked with food source dynamics (Raymont, 1983). Spawning of the (largely) herbivorous *T. inermis* tends to coincide with the spring phytoplankton bloom in May-June (Dalpadado & Skjoldal, 1996), and they can aggregate in areas with high phytoplankton concentrations (Dalpadado et al.,

2016). In fact, most of the guts of euphausiids collected were green, indicating recent feeding on phytoplankton (pers. obs.). The correspondence analysis showed that euphausiids and chaetognaths were strongly associated with greater depths. Data collected over a time series of 1984-1992 revealed high abundances of *T. inermis* and *T. longicaudata* in the deeper AW and adjoining slope area south and south-east of Svalbard Bank during winter and spring (Dalpadado & Skjoldal, 1996). *E. hamata,* the dominating chaetognath species in our samples, has previously been described as a deep-water species (Dvoretsky & Dvoretsky, 2017). Although there is limited knowledge on the role of chaetognaths in Barents Sea, they are major predators on copepods and have been linked to high mortality rates of *Calanus* spp. (Basedow et al., 2014), while usually residing at depths below the maximum concentration of copepods (Samemoto, 1987). The high numbers of chaetognaths may have also contributed to low copepod abundances in our samples, as well as the high mortality of copepods at PF1. This shows that other factors (i.e. resource availability, feeding mode, reproductive cycle, depth) may also be critical for determining species-specific abundances south of the PF.

Macrozooplankton composition in the Arctic Water

Despite sampling being limited in the ArW, several cold water and ice-associated species appeared at PF5 and PF6 (T ∼ -1.5 °C), while AW-associated species were more limited in the ArW. Copepods, amphipods, and pteropods were mostly associated with higher latitudes and shallower sampling stations. Species restricted to PF5 and PF6 were several types of (hyperiid) amphipods (*T. libellula*, *T. abyssorum, H. medusarum,* and *A. glacialis*), pteropods (*L. helicina*), siphonophores, and polar cod larvae, all of which have Arctic or Arctic-boreal distributions (*Appendix II, Table 5*). *T. libellula, C. glacialis, C. hyperboreus,* and *C. limacina* have also been suggested to be good indicator species for ArW (Søreide et al., 2003). The macrozooplankton distributional gradient between the AW and ArW stations indicated by Tucker Trawl data was supported by sharp gradients in beta diversity associated with shifts in water mass properties (Appendix II, *Figure 20*). The beta diversity at PF6 was significantly different ($p < 0.01$) from the rest of the stations and had the highest proportion of species replacement (39.1%), while the overall beta diversity could mostly be explained by a proportional difference in species richness (60.9%). Additionally, stations with small differences in richness (PF2-PF5) are in line with a close association among richness, deeper AW sampling stations, and euphausiids from the correspondence analysis. Although these quantitative measurements should be taken with care because of an uneven sampling distribution across water masses (limited sampling in the ArW), the results provide a good base for combination with future results on the macrozooplankton distribution across the AW and ArW masses.

PF6 was dominated in abundance by herbivorous copepods characteristic of ArW (mainly *C. glacialis* and *C. hyperboreus*) and fewer carnivorous species (e.g. amphipods, gelatinous zooplankton), which coincided with the early phytoplankton bloom stage at this site. Phytoplankton can be considered as a resource proxy that impacts the distribution of herbivorous copepods (Dvoretsky & Dvoretsky, 2017), and has shown here to affect the

distribution of *Calanus* spp. in the ArW. *Themisto* amphipods, known to prey extensively on calanoid copepods (Scott et al., 1999), were also associated with the shallower sampling depth at PF6, and *T. libelulla* generally occurs nearer to the surface than *T. abyssorum* (Dalpadado et al., 2001). High abundances of *T. libellula* have been recorded in the PF region in May-June 1987 and July 1988, and breeding has been suggested to occur here as well (Dalpadado et al., 2001). However, amphipod (and other carnivorous zooplankton) biomass was relatively low in our samples, though this may be compensated as the copepod bloom further progresses. Overall, the moderate copepod bloom near the surface of the ArW was likely an example of a better "match" situation with phytoplankton (in contrast to a string of mismatches in the AW), and these conditions influenced species-specific abundances in correspondence to their feeding modes.

Macrozooplankton data and sampling design

The macrozooplankton compositional structure was successfully resolved from the Tucker trawl, although the acoustic backscatter intensity did not always correspond with trawl data. For example, backscatter was strong at PF5 at near-bottom depths, but Tucker trawl sampling did not reflect the magnitude of the signal. This could possibly be explained by organisms residing closer to the bottom at depths inaccessible to sampling, a known feature to euphausiids (Dalpadado & Skjoldal, 1996). Some of the variability observed in abundance among sampling stations may also be the result of patchiness (Hammer, 1988; Våge et al., 2014), as described earlier. Finally, visual avoidance of nets by highly motile organisms, such as euphausiids and amphipods (Dalpadado & Skjoldal, 1991), even with the large opening of the Tucker trawl (1 m^2), could reduce catches where population densities are high.

Despite the few limitations related to sampling design, the significant association of water-mass distribution with macrozooplankton community composition is in good agreement with previous studies conducted on zooplankton distribution in the Barents Sea (e.g. Arashkevich et al., 2002; Søreide et al., 2003; Eiane & Tande, 2009). Our results further indicate that hydrographical variability is not the only determinant of macrozooplankton biomass found in the PF area, but that other factors (e.g. feeding mode, resource availability, reproductive cycle, depth) contributed to the observed biomass as well. Overall, hydrographic conditions and the thermohaline properties of the PF were important in regulating the latitudinal macrozooplankton assemblage, while biological and environmental factors strongly influenced species-specific abundances.

4.2   Distribution and diet of planktivorous fish

*T*he diets of planktivorous capelin and polar cod assessed in this study are affected by a multitude of factors, such as the foraging area, local prey availability, and gape size, and can fluctuate on a seasonal and interannual basis (Aune et al., 2021; Renaud et al., 2012). The

current state of knowledge on such critical determinants in dietary structure could help explain how the PF may serve an important role to these fish. Stomach content analysis, which has been used as a classical approach throughout decades to explore trophic structure (Amundsen & Sánchez-Hernández, 2019; Buckland et al., 2017), was used in the present study to assess the interactions between macrozooplankton prey and planktivorous fish in the pelagic zone of the PF region. Although extensive ice coverage prevented sampling in the ArW, the current findings on compositional dietary structure and foraging effort provide a snapshot on how macrozooplankton prey distribution and accumulation south of the PF contributes to the diet (*Figure 18*).

Fish distribution

Results from the pelagic trawl showed partial overlap in latitudinal distribution between capelin and polar cod along the transect. Capelin occurred throughout all stations, though in more limited abundances near the PF, and were mostly dominated by medium-sized (8.0 – 12.7 cm) individuals. Spawning of capelin generally occurs from late March to early April and results in large mortalities, with only very few individuals surviving (Gjøsæter, 1998). During the second quartile of the year, juvenile capelin are largely found throughout the central parts of the Barents Sea up until the ice edge where they feed on zooplankton blooms near the surface. Capelin larvae join the rest of these schools after they are released from their spawning grounds, but remain slightly further south (Olsen et al., 2010). This can explain the large amounts of medium-sized capelin and very few larger (11.0 – 14.6 cm) and smaller (6.8 – 9.5 cm) individuals in our catches. Limited abundances found near the PF could be related to temperature, as trawling at the two northernmost stations (PF4 and PF5) occurred in waters below 0°C, with -0.26°C and -1.46°C, respectively. In fact, the preferred temperature of capelin lies between -1 – 3 °C while they tend to avoid waters at temperatures below -1.5 °C (Ingvaldsen & Gjøsæter, 2013), as they are not known to have freeze-coping mechanisms (Hop & Gjøsæter, 2013). Thus, capelin sampled in this study may have reached its northernmost extent, with the PF acting as a barrier for them in May.

Polar cod occurred in lengths 9.0 – 19.0 cm, and were found at the three most northern stations (PF3 - PF5) at temperatures ranging from 0.29°C – -1.46°C, while being absent from the warmer AW stations (PF1 and PF2) at or above 3.0 °C. Polar cod is a true Arctic species and have been suggested to be found predominantly north of the PF (Hop & Gjøsæter, 2013). Although polar cod can tolerate higher temperatures (Christiansen et al., 1997; Drost et al., 2014), it is thought to actively avoid these areas to reduce competition for food sources with other fish like capelin (Hop & Gjøsæter, 2013). The special adaptation of polar cod to the colder water (anti-freeze proteins) may therefore benefit the species in exploiting food sources closer to the PF, and perhaps in the ArW, although the latter cannot be confirmed in this study.

Prey composition and feeding activity

Prey items identified through stomach content analysis were representative of the prey species present in the environment. Stomach contents largely reflected species sampled in the AW, whereas Arctic species restricted to PF6 (Tucker trawl samples) were absent. An opposing trend in *Figure 11* (high versus low abundances at equivalent sampling stations) was observed between macrozooplankton and fish abundances obtained from the trawls. This could either be a consequence of environmental factors and a patchy distribution (as described earlier), or of predatory effects. Top-down control of zooplankton populations has been documented for these fish, which have the ability to deplete zooplankton locally within a timespan of several days (Dalpadado & Skjoldal, 1996; Hop et al., 1997). Despite this not showing up directly in the stomach contents, it is possible that the (often highly digested) prey had already been consumed further ahead of sampling, as our study only provides a snapshot of the feeding patterns.

The stomach content analysis showed considerable overlap in relative prey composition, though this conclusion is tentative given the difference in stomach fullness between both species across stations PF3 and PF4. Euphausiids, which were generally abundant throughout the region (except for PF3), constituted the main prey item for both polar cod (62.0 – 96.4 %IRI) and capelin (16.5 – 76.55 %IRI), especially larger capelin above ~12 cm at PF5 ($p < 0.05$ %N). Copepods were the second most important prey item in polar cod (0.46 – 37.6 %IRI) and capelin (0 – 54.0 %IRI), and showed a substantial contribution to the stomach contents of capelin below ~12 cm at PF5 ($p < 0.05$ %N). Teleosts (mainly capelin) were found in the stomachs of large polar cod (>13 cm) at PF4 and PF5. These results imply a size-dependent feeding behaviour, with copepods being more frequently consumed by smaller-sized fish, and larger food items (e.g. euphausiids and teleosts) being preferred as fish grow (Ajiad & Gjøsæter, 1990; Renaud et al., 2012; Dalpadado & Mowbray, 2013).

Data collected during earlier dietary studies and contribution of euphausiids to the diet of polar cod demonstrated similar findings. Polar cod sampled in the central parts of the Barents Sea in 1986-1988 showed a high percentage of euphausiids in terms of relative weight compared to the north-eastern and south-eastern parts, especially in individuals <14 cm (Ajiad & Gjøsæter, 1990). Additionally, euphausiids (followed by copepods) dominated the diet of adult polar cod (63.1%) in samples from May 1969 in the eastern parts of the Barents Sea, although feeding intensity remained low until June (Aune et al., 2021). By way of contrast, data from another study on samples collected in Svalbard waters pointed out a high probability of filled stomachs in May (Cusa, 2016). The ambiguity of feeding intensity can be attributed to seasonal and spatial variation in prey availability (Aune et al., 2021). In our study, no polar cod had empty stomachs. The overall stomach fullness was >30% and highest near the PF (43.3%). The total prey frequency ranged between 1-17 prey items, which indicates that most polar cod were actively feeding across stations they were found. Polar cod as a generalist predator (Renaud et al., 2012) may also exhibit opportunistic behaviour due to its diet plasticity in adaptations to altering prey availability and habitat heterogeneity (Cusa,
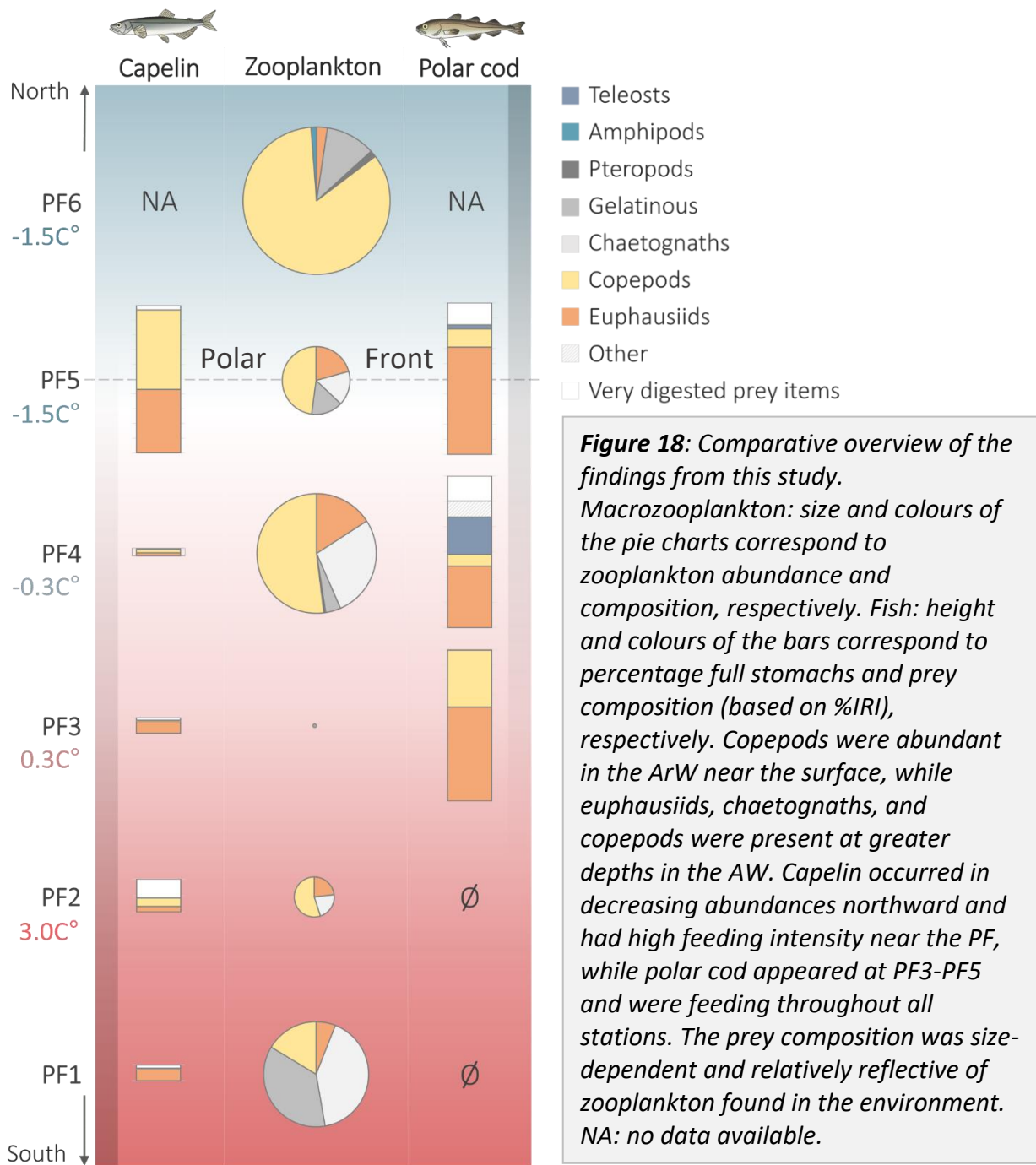
2016; Cusa et al., 2019). This trait could have benefitted polar cod by taking advantage of food sources passed the PF in the AW. The results presented here suggest that the PF area can be used as a feeding ground for polar cod in spring.

Grazing upon euphausiids by capelin is common during the months February-May, especially among adults (Gjøsæter, 1998; Orlova et al., 2013), which is generally reflected in our findings. Our results also showed significantly higher feeding activity of capelin closest to the PF (PF5, $p < 0.05$) compared to the more southerly stations (PF1 – PF4), this despite their general avoidance of sub-zero waters. The high percentage of empty capelin stomachs across PF1 – PF4 could be attributed to the fact that copepods, which were more important to the dominating smaller-sized capelin in our samples, were found in low abundances across most of the AW stations. On the contrary, the presence of the small copepod bloom in the ArW may signify that the 'capelin front' is still shifting northwards as the ice continues to break up and melt, and as it is well known that annual feeding migrations lead the capelin north of the PF later in the season (Hop & Gjøsæter, 2013). Depth distribution may have also played a significant role, since capelin were mostly observed in the shallower waters at stations PF1-PF4 (Appendix II, *Figure 21*), while they occurred closer to the bottom at PF5 where euphausiids were abundant. The effect of vertical migrations by capelin on depth distribution could likely be diminished, as these become less distinct and not clearly diurnal during the 24-hour daylight cycle (Gjøsæter, 1998). Capelin may have seeked shallow waters at preferred temperatures from the sun heating up the surface layers (Methven & Piatt, 1991), or to avoid competition for similar food sources and predation by other fish (Hop & Gjøsæter, 2013), since capelin occurred in polar cod stomachs. Capelin caught near the seabed are often larger than capelin caught at shallow and intermediate depths (Olsen et al., 2010), and large-sized capelin were shown to feed more commonly on euphausiids in our research. In fact, another study also found higher feeding intensities at greater depths where prey (mainly euphausiids) aggregated during the daylight (Orlova et al., 2009). Overall, high feeding activity near the PF suggests that the PF area can be utilized as a feeding ground by capelin, but a greater temporal resolution is required to see if this pattern continues for the large schools over time.

Stomach content data and sampling design
While the main goal of any scientific study is to reflect the reality as close as possible, any methodology only reflects this partially and may come with certain biases. For example, the numerical method may lead to overestimation of small prey (e.g. copepods) and non-digestible components, while the relative-fullness method may not always represent nutritional value, especially of prey items with large volumes of water (gelatinous organisms) or extensive exoskeletons. Additionally, easily digestible food items, such as gelatinous zooplankton, can be difficult for detection by visual assessment alone and may need complementary DNA-analysis (Buckland et al., 2017; Amundsen & Sánchez-Hernández, 2019; Sagar et al., 2019). High abundances of chaetognaths from the Tucker trawl samples may have therefore gone undetected in the stomach contents. However, chaetognaths are less

preferred food items to planktivorous fish, as they can negatively affect body fatness (Orlova et al., 2009). Other approaches, such as the gravimetric method (based on prey item weight), may be more precise but can be very time-consuming and impossible to manage under rough circumstances at sea or with very small fish. Nevertheless, the overall strength in assessing stomach contents lies in a combination of several approaches. Here we used the stomach fullness, the numerical method, the frequency-occurrence, and the relative-fullness methods, which have been reviewed and recommended as a quick yet solid approach to obtain reliable results on dietary structure (Buckland et al., 2017; Amundsen & Sánchez-Hernández, 2019). These were be used to estimate factors such as foraging activity and relative prey composition through calculation of relevant indices like %IRI (Sagar et al., 2019). Other methods were reviewed and a more detailed analysis on this can be found in *Table 4* (Appendix I).

Figure 18: Comparative overview of the findings from this study. Macrozooplankton: size and colours of the pie charts correspond to zooplankton abundance and composition, respectively. Fish: height and colours of the bars correspond to percentage full stomachs and prey composition (based on %IRI), respectively. Copepods were abundant in the ArW near the surface, while euphausiids, chaetognaths, and copepods were present at greater depths in the AW. Capelin occurred in decreasing abundances northward and had high feeding intensity near the PF, while polar cod appeared at PF3-PF5 and were feeding throughout all stations. The prey composition was size-dependent and relatively reflective of zooplankton found in the environment. NA: no data available.

Findings on the dietary structure and feeding activity elucidate and support the suggestion that the PF should be considered a more complex system, with multiple oceanographic features contributing to the diet and (enhanced) feeding activity in the PF area during spring. The findings showed that preference and tolerance to AW temperatures and prey distribution regulated the distribution and feeding patterns of pelagic fish south of the PF. Stomach contents were reflective of macrozooplankton found in the environment: euphausiids and copepods constituted important prey for both fish, while capelin were also frequently consumed by polar cod. The dominating medium-sized class of capelin, which were found to consume copepods more frequently, coincided with low copepod prey abundances across most of the AW stations, and this was likely responsible for the high percentages of empty capelin stomachs. However, high feeding activity on macrozooplankton prey accumulations south of the PF let us to conclude that both planktivorous fish can utilize the PF as a feeding ground. Overall, the biological observations associated with the PF and MW front during spring were intertwined, but the co-occurrence of these fronts has been shown to contribute each considerably to the distribution and feeding behaviour of capelin and polar cod.

4.3   Climate change and future perspectives for the PF, macrozooplankton, and fish

*C*limate change effects will likely affect standing stocks and ecological interactions at the PF. Two commonly used terms in the literature related to climate change impacts are 'Atlantification', which is associated with a stronger influx of AW into the Barents Sea, and 'borealization', which refers to the northward expansion of boreal species into the Arctic regions (Ingvaldsen et al., 2021). In the case of the PF, the majority of the ecological changes in the foreseeable future will be the product of physical manifestations surrounding the PF system, with 1) the thermohaline barrier being a relatively stable feature in the west (in contrast to the eastern salinity and temperature branches) (Oziel et al., 2016), and 2) alterations in sea-ice cover impacting the MW front (Leu et al., 2011). To which extent these features may impact the dynamics between zooplankton and planktivorous fish at the PF depends on various factors, which are briefly highlighted below.

Various studies point out an increased inflow of AW resulting from warmer temperatures leading to greater advection of zooplankton organisms into the Barents Sea, including that of boreal euphausiids and *C. finmarchicus* becoming increasingly dominant (Dalpadado et al., 2003; Wassmann et al., 2006). Meanwhile, capelin exert a strong predation pressure over the euphausiid abundance in the Barents Sea (Dalpadado et al., 2003; Orlova et al., 2010), and have been suspected a shift in spatial patterns northwards as temperatures increase (Ingvaldsen & Gjøsæter, 2013; Orlova et al., 2013). Climatic changes leading to alterations in euphausiid abundance vary on a regional basis, but the predatory effect of capelin on euphausiids could become more significant in the ArW over time, which may intensify the euphausiid-capelin link (Orlova et al., 2015). An increased advection of

euphausiids could provide a buffer to fluctuations in prey availability, which may also sustain other boreal planktivores if they were to expand their distribution northwards (Orlova et al., 2015). We saw evidence of this in the presence (and consumption) of euphausiids in spring when *Calanus* populations were low. In recent times with high euphausiid and low capelin abundances, other pelagic fish stocks (e.g. polar cod, juvenile herring, blue whiting) increased to fill the 'capelin gap' (Eriksen et al., 2017). While conceivably the main threat to polar cod is the loss of its sympagic habitat (Huserbråten et al., 2019), the generalistic and opportunistic feeding behaviour of polar cod may benefit the species in adapting to other food sources, including an increased availability of euphausiids. However, enhanced competition between capelin and polar cod may affect capelin negatively (Orlova et al., 2009), while northwards expansion and increased predation of polar cod by boreal taxa (e.g. Atlantic cod and haddock) may negatively impact polar cod abundances (Renaud et al., 2012). In general, borealization increases food web connectivity that may be accompanied by greater competition, while Arctic food webs were previously characterized by a few specialized species contributing to fewer links to the food web (Kortsch et al., 2015; Ingvaldsen et al., 2021). Thus, accumulations of prey organisms near the thermohaline boundary may continue to be important for maintaining planktivorous fishes in the future. It may even become more significant with an increase of advected organisms and northwards expansion of boreal fish. In spite of this, borealization of fish communities and greater prey availability may also lead to increased competition in our area of study, while colder temperatures associated with the ArW may prevent non-adapted species from migrating further north.

Concurrently, a regime shift in timing of algal blooms, algal food quality, and reproduction and growth cycles of *C. glacialis* is expected to occur as a consequence of reductions in sea-ice thickness and coverage. The earlier break up of sea-ice will likely impact the onset of the phytoplankton bloom, potentially causing a mismatch to become more common between algal food sources and key Arctic grazers, with further impacts on the energy transfer to higher trophic levels (Søreide et al., 2010). We saw evidence of this mismatch during our cruise in May 2022, and during a similar cruise to the area in May 2021 (P. Renaud, Akvpalan-niva, pers. comm.). The low copepod abundance associated with this had negative consequences on food availability for smaller-sized fish. In the (near) future, secondary production by *C. glacialis* is expected to decline by 90%, compared to a 3-fold increase for *C. finmarchicus* (Slagstad et al., 2011). Meanwhile, Arctic *Calanus spp.* have a higher lipid-content (60-70 mass %) than *C. finmarchicus* (30-50 mass %) (Scott et al., 2000), and thus a valuable energy source may be lost as climate warming proceeds. A higher energy expenditure by capelin may be required to continue the annual feeding and spawning migrations (Hop & Gjøsæter, 2013), although this may be more prevalent in the eastern Barents Sea where the retraction of the ice extend has been greater throughout the years (Ingvaldsen et al., 2021). However, the expected decrease in abundance and higher lipid content of *C. glacialis* could potentially be compensated by the increase in abundance and higher turnover rate of *C. finmarchicus* (Renaud et al., 2018). Nevertheless, a new

zooplankton regime would require adjustments by planktivorous fish to timing and alterations in availability of suitable prey. Examples could be the establishment new spawning grounds in the north to offset the longer migration distances for capelin (Hop & Gjøsæter, 2013), as well as intensified foraging effort on *C. finmarchicus* to counterbalance for its lower nutritional value.

Despite some positive indications that certain planktivorous fish may (continue to) benefit from increased advection and accumulation of organisms near the PF, copepods are a critical food source for younger fish stages, which may be threatened by climatic changes related to the MW front. Factors including timing and availability of suitable zooplankton prey, as well as size-dependent feeding behaviour, dietary preferences, and a possible increased competition and predation by (other) boreal species will ultimately determine how planktivorous species will react to climate changes at the PF. To get a better understanding on the role of the PF in critical times with major shifts in ecosystems, a finer temporal and seasonal resolution is necessary, which will be provided by forthcoming data from the winter and summer seasons. An extended analysis on macrozooplankton assemblage and water mass distribution in comparison with previous studies could point out potential changes in community structures over time. Additionally, a seasonal comparison with the present dietary data is needed to see if feeding patterns change during the polar night and summer, two seasons known for their low high feeding activity, respectively. Ultimately, the larger dataset will give a better indication on how the Arctic ecosystem may evolve in a progressing Atlantification scenario.

5   CONCLUSIONS

*T*his study has significantly advanced our understanding on the macrozooplankton distribution and feeding ecology of pelagic fish across the Barents Sea PF in spring 2022. Two main co-occurring oceanographic features dominated the area, namely the thermohaline barrier imposed by the PF, as well as the more dynamic and seasonally occurring MW front, induced by melting ice that passed onto the warmer Atlantic side of the PF.

The PF, considered primarily as a passive front, acted as a strong biological boundary and was a critical determinant in structuring latitudinal species communities. The AW and ArW masses were characterized by distinct taxonomic compositions, and the macrozooplankton community was most diverse just south of the PF in the AW. The early onset of an intense phytoplankton bloom related to the MW front coincided with low abundances of herbivorous copepods, showing an example of a mismatch scenario. Overall, hydrographical conditions and other factors (i.e. resource availability, feeding mode, reproductive cycle, depth) were responsible for community structure, patchy distributions, and observed accumulation of macrozooplankton in the PF area.

Temperature sensitivity and prey distribution influenced the distribution and diet of capelin and polar cod south of the PF. Capelin, dominated by juveniles, occurred at all stations but in limiting abundances closer to the PF, while polar cod occurred south of the PF mainly at temperatures around or below 0 °C. The main prey for capelin and polar cod reflected macrozooplankton sampled in the AW and included euphausiids and copepods, while teleosts were also important dietary components for polar cod. Both species benefitted from feeding near the PF, as high foraging activity was reported in this area. Capelin exhibited a size-dependent feeding behaviour, where copepods and euphausiids were more common in smaller- and larger-sized fish, respectively. However, high percentages of empty capelin stomachs further south concurred with low abundances of herbivorous copepods in the environment. Overall, the unpredictable nature of the MW front in spring that coincided with low copepod prey abundances had negative consequences on the diet of smaller planktivorous fish south of the PF, whereas advected and aggregating organisms near the PF could potentially serve a continuous food source (over time).

In the context of climate change and progressing Atlantification, an increased advection of zooplankton, an altered timing and regime of copepod blooms, and a northwards expansion of boreal species can be expected. This requires adaptations of planktivorous fish to alterations in timing and availability of suitable zooplankton prey, while coping with increased levels of predation and competition in the PF area. A finer temporal and seasonal resolution is needed to extend the currents findings and to see how species distribution and feeding patterns may change throughout the year.

ACKNOWLEDGEMENT

REFERENCES

Ajiad, A. M., & Gjøsæter, H. (1990). Diet of polar cod, Boreogadus saida, in the Barents Sea related to fish size and geographical distribution. In *9 s.* [Working paper]. ICES. https://imr.brage.unit.no/imr-xmlui/handle/11250/104775

Amundsen, P.-A., & Sánchez-Hernández, J. (2019). Feeding studies take guts – critical review and recommendations of methods for stomach contents analysis in fish. *Journal of Fish Biology*, *95*(6), 1364–1373. https://doi.org/10.1111/jfb.14151

Arashkevich, E., Wassmann, P., Pasternak, A., & Wexels Riser, C. (2002). Seasonal and spatial changes in biomass, structure, and development progress of the zooplankton community in the Barents Sea. *Journal of Marine Systems*, *38*(1), 125–145. https://doi.org/10.1016/S0924-7963(02)00173-2

Aune, M., Raskhozheva, E., Andrade, H., Augustine, S., Bambulyak, A., Camus, L., Carroll, J., Dolgov, A. V., Hop, H., Moiseev, D., Renaud, P. E., & Varpe, Ø. (2021). Distribution and ecology of polar cod (Boreogadus saida) in the eastern Barents Sea: A review of historical literature. *Marine Environmental Research*, *166*, 105262. https://doi.org/10.1016/j.marenvres.2021.105262

Barton, B. I., Lenn, Y.-D., & Lique, C. (2018). Observed Atlantification of the Barents Sea Causes the Polar Front to Limit the Expansion of Winter Sea Ice. *Journal of Physical Oceanography*, *48*(8), 1849–1866. https://doi.org/10.1175/JPO-D-18-0003.1

Basedow, S. L., Zhou, M., & Tande, K. S. (2014). Secondary production at the Polar Front, Barents Sea, August 2007. *Journal of Marine Systems*, *130*, 147–159. https://doi.org/10.1016/j.jmarsys.2013.07.015

Belkin, I. M. (2021). Remote Sensing of Ocean Fronts in Marine Ecology and Fisheries. *Remote Sensing*, *13*(5), 883. https://doi.org/10.3390/rs13050883

Belkin, I. M., Cornillon, P., & Sherman, K. (2009). Fronts in Large Marine Ecosystems. *Progress in Oceanography - PROG OCEANOGR*, *81*, 223–236. https://doi.org/10.1016/j.pocean.2009.04.015

Bluhm, B., Hop, H., Melnikov, I., Poulin, M., Vihtakari, M., Collins, R., Gradinger, R., Juul-Pedersen, T., & Quillfeldt, C. (2017). Sea Ice Biota. In *State of the Arctic Marine Biodiversity Report* (pp. 33–61). Conservation of Arctic Flora and Fauna International Secretariat.

Buckland, A., Baker, R., Loneragan, N., & Sheaves, M. (2017). Standardising fish stomach content analysis: The importance of prey condition. *Fisheries Research*, *196*, 126–140. https://doi.org/10.1016/j.fishres.2017.08.003

Cairns, S., Calder, D., Brinckmann-Voss, A., Castro, C., Fautin, D., Pugh, P., Mills, C., Jaap, W., Arai, M., Haddock, S., & Opresko, D. (2002). *Common and scientific names of aquatic invertebrates from the United States and Canada: Cnidaria and Ctenophora. 2nd ed*. https://doi.org/10.47886/9781888569643

Carmack, E., Barber, D., Christensen, J., Macdonald, R., Rudels, B., & Sakshaug, E. (2006). Climate variability and physical forcing of the food webs and the carbon budget on panarctic shelves. *Progress in Oceanography*, *71*(2), 145–181. https://doi.org/10.1016/j.pocean.2006.10.005

Christiansen, J., Schurmann, H., & Larisa, K. (1997). Thermal behaviour of polar fish: A brief survey and suggestions for research. *Cybium*, *21*, 353–362.

Cury, P., Bakun, A., Crawford, R. J. M., Jarre, A., Quiñones, R. A., Shannon, L. J., & Verheye, H. M. (2000). Small pelagics in upwelling systems: Patterns of interaction and structural changes in "wasp-waist" ecosystems. *ICES Journal of Marine Science*, *57*(3), 603–618. https://doi.org/10.1006/jmsc.2000.0712

Cusa, M. (2016). The effect of seasonality on polar cod (Boreogadus saida) dietary habits and temporal feeding strategies in Svalbard waters. *Undefined*. https://www.semanticscholar.org/paper/The-effect-of-seasonality-on-polar-cod-(Boreogadus-Cusa/69552e93f0ed50d70634e7cab9cb387650a6ddb6

Cusa, M., Berge, J., & Varpe, Ø. (2019). Seasonal shifts in feeding patterns: Individual and population realized specialization in a high Arctic fish. *Ecology and Evolution*, *9*(19), 11112–11121. https://doi.org/10.1002/ece3.5615

Daase, M., Berge, J., Søreide, J. E., & Falk-Petersen, S. (2021). Ecology of Arctic Pelagic Communities. In *Arctic Ecology* (pp. 219–259). John Wiley & Sons, Ltd. https://doi.org/10.1002/9781118846582.ch9

Daase, M., Varpe, Ø., & Falk-Petersen, S. (2014). Non-consumptive mortality in copepods: Occurrence of Calanus spp. carcasses in the Arctic Ocean during winter. *Journal of Plankton Research*, *36*(1), 129–144. https://doi.org/10.1093/plankt/fbt079

Dalpadado, P., Arrigo, K., Hjøllo, S., Rey, F., Ingvaldsen, R., Sperfeld, E., van Dijken, G., Stige, L., Olsen, A., & Ottersen, G. (2014). Productivity in the Barents Sea—Response to Recent Climate Variability. *PloS One*, *9*, e95273. https://doi.org/10.1371/journal.pone.0095273

Dalpadado, P., Borkner, N., Bogstad, B., & Dalpadado, S. (2001). Distribution of Themisto (Amphipoda) spp. In the Barents Sea and predator-prey interactions. *ICES Journal of Marine Science*, *58*, 876–895. https://doi.org/10.1006/jmsc.2001.1078

Dalpadado, P., Hop, H., Rønning, J., Pavlov, V., Sperfeld, E., Buchholz, F., Rey, A., & Wold, A. (2016). Distribution and abundance of euphausiids and pelagic amphipods in Kongsfjorden, Isfjorden and Rijpfjorden (Svalbard) and changes in their relative importance as key prey in a warming marine ecosystem. *Polar Biology*, *39*(10), 1765–1784. https://doi.org/10.1007/s00300-015-1874-x

Dalpadado, P., Ingvaldsen, R. B., Stige, L. C., Bogstad, B., Knutsen, T., Ottersen, G., & Ellertsen, B. (2012). Climate effects on Barents Sea ecosystem dynamics. *ICES Journal of Marine Science*, *69*(7), 1303–1316. https://doi.org/10.1093/icesjms/fss063

Dalpadado, P., Ingvaldsen, R., & Hassel, A. (2003). Zooplankton biomass variation in relation to climatic conditions in the Barents Sea. *Polar Biology*, *26*, 233–241. https://doi.org/10.1007/s00300-002-0470-z

Dalpadado, P., & Mowbray, F. (2013). Comparative analysis of feeding ecology of capelin from two shelf ecosystems, off Newfoundland and in the Barents Sea. *Progress in Oceanography*, *114*, 97–105. https://doi.org/10.1016/j.pocean.2013.05.007

Dalpadado, P., & Skjoldal, H. R. (1991). Distribution and life history of krill from the Barents Sea. *Polar Research*, *10*(2), 443–460. Scopus. https://doi.org/10.1111/j.1751-8369.1991.tb00665.x

Dalpadado, P., & Skjoldal, H. R. (1996). Abundance, maturity and growth of the krill species Thysanoessa inermis and T. longicaudata in the Barents Sea. *Marine Ecology Progress Series*, *144*, 175–183. https://doi.org/10.3354/meps144175

Dalpadado, P., Yamaguchi, A., Ellertsen, B., & Johannessen, S. (2008). Trophic interactions of macro-zooplankton (krill and amphipods) in the Marginal Ice Zone of the Barents Sea. *Deep Sea Research Part II: Topical Studies in Oceanography*, *55*(20), 2266–2274. https://doi.org/10.1016/j.dsr2.2008.05.016

Drinkwater, K., & Tande, K. (2014). Biophysical studies of the Polar Front in the Barents Sea and the Arctic Front in the Norwegian Sea: Results from the NESSAR Project. *Journal of Marine Systems*, *130*, 131–133. https://doi.org/10.1016/j.jmarsys.2013.11.011

Drost, H. E., Carmack, E. C., & Farrell, A. P. (2014). Upper thermal limits of cardiac function for Arctic cod Boreogadus saida, a key food web fish species in the Arctic Ocean. *Journal of Fish Biology*, *84*(6), 1781–1792. https://doi.org/10.1111/jfb.12397

Dvoretsky, V., & Dvoretsky, A. (2017). Macrozooplankton of the Arctic – The Kara Sea in relation to environmental conditions. *Estuarine, Coastal and Shelf Science*, *188*, 38–55. https://doi.org/10.1016/j.ecss.2017.02.008

Edvardsen, A., Slagstad, D., Tande, K., & Jaccard, P. (2003). Assessing zooplankton advection in the Barents Sea using underway measurements and modelling. *Fisheries Oceanography*, *12*, 61–74. https://doi.org/10.1046/j.1365-2419.2003.00219.x

Eiane, K., & Tande, K. S. (2009). Meso and macrozooplankton. In *Ecosystem Barents Sea* (p. 596). Tapir Academic Press.

Engelsen, O., Hegseth, E. N., Hop, H., Hansen, E., & Falk-Petersen, S. (2002). Spatial variability of chlorophyll-a in the Marginal Ice Zone of the Barents Sea, with relations to sea ice and oceanographic conditions. *Journal of Marine Systems*, *35*(1), 79–97. https://doi.org/10.1016/S0924-7963(02)00077-5

Eriksen, E., Benzik, A. N., Dolgov, A. V., Skjoldal, H. R., Vihtakari, M., Johannesen, E., Prokhorova, T. A., Keulder-Stenevik, F., Prokopchuk, I., & Strand, E. (2020). Diet and trophic structure of fishes in the Barents Sea: The Norwegian-Russian program "Year of stomachs" 2015 – Establishing a baseline. *Progress in Oceanography*, *183*, 102262. https://doi.org/10.1016/j.pocean.2019.102262

Eriksen, E., Skjoldal, H. R., Dolgov, A. V., Dalpadado, P., Orlova, E. L., & Prozorkevich, D. V. (2016). The Barents Sea euphausiids: Methodological aspects of monitoring and estimation of abundance and biomass. *ICES Journal of Marine Science*, *73*(6), 1533–1544. https://doi.org/10.1093/icesjms/fsw022

Eriksen, E., Skjoldal, H. R., Gjøsæter, H., & Primicerio, R. (2017). Spatial and temporal changes in the Barents Sea pelagic compartment during the recent warming. *Progress in Oceanography*, *151*, 206–226. https://doi.org/10.1016/j.pocean.2016.12.009

Falk-Petersen, S., Hop, H., Budgell, W. P., Hegseth, E., Korsnes, R., Løyning, T., Ørbæk, J., Kawamura, T., & Shirasawa, K. (2000). Physical and ecological processes in the marginal ice zone of the northern Barents Sea during the summer melt period. *Journal of Marine Systems*, *27*, 131–159. https://doi.org/10.1016/S0924-7963(00)00064-6

Falk-Petersen, S., Hopkins, C., & Sargent, J. R. (1990). Trophic relationships in the pelagic, Arctic food web. *Trophic Relationships in the Marine Environment*, 315–333.

Falk-Petersen, S., Mayzaud, P., Kattner, G., & Sargent, J. R. (2009). Lipids and life strategy of Arctic Calanus. *Marine Biology Research*, *5*(1), 18–39. https://doi.org/10.1080/17451000802512267

Fer, I., & Drinkwater, K. (2014). Mixing in the Barents Sea Polar Front near Hopen in spring. *Journal of Marine Systems*, *130*, 206–218. https://doi.org/10.1016/j.jmarsys.2012.01.005

Fossheim, M., Primicerio, R., Johannesen, E., Ingvaldsen, R. B., Aschan, M. M., & Dolgov, A. V. (2015). Recent warming leads to a rapid borealization of fish communities in the Arctic. *Nature Climate Change*, *5*(7), 673–677. https://doi.org/10.1038/nclimate2647

Frank, K. T., Petrie, B., & Shackell, N. L. (2007). The ups and downs of trophic control in continental shelf ecosystems. *Trends in Ecology & Evolution*, *22*(5), 236–242. https://doi.org/10.1016/j.tree.2007.03.002

Franks, P. (1992). Sink or swim, accumulation of biomass at fronts. *Marine Ecology Progress Series*, *82*, 1–12. https://doi.org/10.3354/meps082001

Geoffroy, M., Robert, D., Darnis, G., & Fortier, L. (2011). The aggregation of polar cod (Boreogadus saida) in the deep Atlantic layer of ice-covered Amundsen Gulf (Beaufort Sea) in winter. *Polar Biology*, *34*(12), 1959–1971. https://doi.org/10.1007/s00300-011-1019-9

Gjøsæter, H. (1998). The population biology and exploitation of capelin (Mallotus villosus) in the barents sea. *Sarsia*, *83*(6), 453–496. https://doi.org/10.1080/00364827.1998.10420445

Gjøsæter, H. (2000). *Studies on the Barents Sea Capelin (Mallotus villosus Müller), with emphasis on growth*. https://doi.org/10.13140/RG.2.1.3153.8647

Hagen, W. (1999). Reproductive strategies and energetic adaptations of polar zooplankton. *Invertebrate Reproduction & Development*, *36*(1–3), 25–34. https://doi.org/10.1080/07924259.1999.9652674

Hammer, W. (1988). Behavior of plankton and patch formation in pelagic ecosystems. *Undefined*. https://www.semanticscholar.org/paper/Behavior-of-plankton-and-patch-formation-in-pelagic-Hammer/bc0a137df40a9dd213884ce4bd9f96cffc5b67f5

Harris, C. L., Plueddemann, A. J., & Gawarkiewicz, G. G. (1998). Water mass distribution and polar front structure in the western Barents Sea. *Journal of Geophysical Research: Oceans*, *103*(C2), 2905–2917. https://doi.org/10.1029/97JC02790

Hassel, A., Skjoldal, H. R., Gjøsæter, H., Loeng, H., & Omli, L. (1991). Impact of grazing from capelin (Mallotus villosus) on zooplankton: A case study in the northern Barents Sea in August 1985. *Polar Research*, *10*(2), 371–388. https://doi.org/10.3402/polar.v10i2.6753

Hirche, H.-J., & Kattner, G. (1993). Egg production and lipid content of Calanus glacialis in spring: Indication of a food-dependent and food-independent reproductive mode. *Marine Biology*, *117*(4), 615–622. Scopus. https://doi.org/10.1007/BF00349773

Hoegh-Guldberg, O., & Bruno, J. F. (2010). The Impact of Climate Change on the World's Marine Ecosystems. *Science*, *328*(5985), 1523–1528. https://doi.org/10.1126/science.1189930

Hop, H., & Gjøsæter, H. (2013). Polar cod (Boreogadus saida) and capelin (Mallotus villosus) as key species in marine food webs of the Arctic and the Barents Sea. *Marine Biology Research*, *9*(9), 878–894. https://doi.org/10.1080/17451000.2013.775458

Hop, H., Welch, H., & Crawford, R. (1997). *Population structure and feeding ecology of Arctic cod schools in the Canadian High Arctic.*

Huserbråten, M. B. O., Eriksen, E., Gjøsæter, H., & Vikebø, F. (2019). Polar cod in jeopardy under the retreating Arctic sea ice. *Communications Biology*, *2*(1), 1–8. https://doi.org/10.1038/s42003-019-0649-2

Ingvaldsen, R. B., Assmann, K. M., Primicerio, R., Fossheim, M., Polyakov, I. V., & Dolgov, A. V. (2021). Physical manifestations and ecological implications of Arctic Atlantification. *Nature Reviews Earth & Environment*, *2*(12), 874–889. https://doi.org/10.1038/s43017-021-00228-x

Ingvaldsen, R. B., & Gjøsæter, H. (2013). Responses in spatial distribution of Barents Sea capelin to changes in stock size, ocean temperature and ice cover. *Marine Biology Research*, *9*(9), 867–877. https://doi.org/10.1080/17451000.2013.775450

Kortsch, S., Primicerio, R., Fossheim, M., Dolgov, A. V., & Aschan, M. (2015). Climate change alters the structure of arctic marine food webs due to poleward shifts of boreal generalists. *Proceedings of the Royal Society B: Biological Sciences*, *282*(1814), 20151546. https://doi.org/10.1098/rspb.2015.1546

Le Fèvre, J. (1987). Aspects of the Biology of Frontal Systems. In J. H. S. Blaxter & A. J. Southward (Eds.), *Advances in Marine Biology* (Vol. 23, pp. 163–299). Academic Press. https://doi.org/10.1016/S0065-2881(08)60109-1

Lee, R., Hagen, W., & Kattner, G. (2006). Lipid storage in marine zooplankton. *Marine Ecology-Progress Series - MAR ECOL-PROGR SER*, *307*, 273–306. https://doi.org/10.3354/meps307273

Legeżyńska, J., Włodarska-Kowalczuk, M., Gluchowska, M., Ormańczyk, M., Kędra, M., & Węsławski, J. M. (2017). The malacostracan fauna of two Arctic fjords (west Spitsbergen): The diversity and distribution patterns of its pelagic and benthic components. *Oceanologia*, *59*(4), 541–564. https://doi.org/10.1016/j.oceano.2017.01.004

Leu, E., Søreide, J. E., Hessen, D. O., Falk-Petersen, S., & Berge, J. (2011). Consequences of changing sea-ice cover for primary and secondary producers in the European Arctic shelf seas: Timing, quantity, and quality. *Progress in Oceanography*, *90*(1), 18–32. https://doi.org/10.1016/j.pocean.2011.02.004

Lien, V. S. (2018). *Polarfrontens fysiske beskaffenhet og biologiske implikasjoner* (Fisken og havet, p. 75). Institute of Marine Research.

Loeng, H. (1991). Features of the physical oceanographic conditions of the Barents Sea. *Polar Research*, *10*(1), 5–18. https://doi.org/10.3402/polar.v10i1.6723

Loeng, H., & Drinkwater, K. (2007). An overview of the ecosystems of the Barents and Norwegian Seas and their response to climate variability. *Deep Sea Research Part II: Topical Studies in Oceanography*, *54*(23), 2478–2500. https://doi.org/10.1016/j.dsr2.2007.08.013

Lønne, O. J., & Gulliksen, B. (1989). Size, age and diet of polar cod, Boreogadus saida (Lepechin 1773), in ice covered waters. *Polar Biology*, *9*(3), 187–191. https://doi.org/10.1007/BF00297174

Mańko, M., Merchel, M., Kwasniewski, S., & Weydmann-Zwolicka, A. (2022). Oceanic Fronts Shape Biodiversity of Gelatinous Zooplankton in the European Arctic. *Frontiers in Marine Science*, *9*, 941025. https://doi.org/10.3389/fmars.2022.941025

Martinetto, P., Alemany, D., Botto, F., Mastrángelo, M., Falabella, V., Acha, E. M., Antón, G., Bianchi, A., Campagna, C., Cañete, G., Filippo, P., Iribarne, O., Laterra, P., Martínez, P., Negri, R., Piola, A. R., Romero, S. I., Santos, D., & Saraceno, M. (2020). Linking the scientific knowledge on marine frontal systems with ecosystem services. *Ambio*, *49*(2), 541–556. https://doi.org/10.1007/s13280-019-01222-w

Methven, D. A., & Piatt, J. F. (1991). Seasonal abundance and vertical distribution of capelin (Mallotus villosus) in relation to water temperature at a coastal site off eastern Newfoundland. In *ICES Journal of Marine Science* (Vol. 48, Issue 2, p. 187193). https://doi.org/10.1093/icesjms/48.2.187

Mundy, C., Ehn, J., Barber, D., & Michel, C. (2007). Influence of snow cover and algae on the spectral dependence of transmitted irradiance through Arctic landfast first-year sea ice. *Journal of Geophysical Research-Oceans*, *112*. https://doi.org/10.1029/2006jc003683

Nenadic, O., & Greenacre, M. (2007). Correspondence Analysis in R, with two- and three-dimensional graphics: The ca package. *Journal of Statistical Software*, *20*(3), 1–13.

Oksanen, J., Simpson, G., Blanchet, F., Legendre, P., Minchin, P., O'Hara, R., Solymos, P., Stevens, M., Szoecs, E., Wagner, H., Barbour, M., Bedward, M., Bolker, B., Borcard, D., Carvalho, G., Chirico, M., De Caceres, M., Durand, S., Evangeslista, H., … Weedon, J. (2022). *vegan: Community Ecology Package*. https://CRAN.R-project.org/package=vegan

Olsen, E., Aanes, S., Mehl, S., Holst, J. C., Aglen, A., & Gjøsæter, H. (2010). Cod, haddock, saithe, herring, and capelin in the Barents Sea and adjacent waters: A review of the biological value of the area. *ICES Journal of Marine Science*, *67*(1), 87–101. https://doi.org/10.1093/icesjms/fsp229

Orlova, E., Dolgov, A., Rudneva, G., Oganin, I., & Konstantinova, L. (2009). Trophic relations of capelin Mallotus villosus and polar cod Boreogadus saida in the Barents Sea as a factor of impact on the ecosystem. *Deep-Sea Research Part Ii-Topical Studies in Oceanography - DEEP-SEA RES PT II-TOP ST OCE*, *56*, 2054–2067. https://doi.org/10.1016/j.dsr2.2008.11.016

Orlova, E. L., Dolgov, A. V., Renaud, P. E., Boitsov, V. D., Prokopchuk, I. P., & Zashihina, M. V. (2013). Structure of the macroplankton–pelagic fish–cod trophic complex in a warmer Barents Sea. *Marine Biology Research*, *9*(9), 851–866. https://doi.org/10.1080/17451000.2013.775453

Orlova, E. L., Dolgov, A. V., Renaud, P. E., Greenacre, M., Halsband, C., & Ivshin, V. A. (2015). Climatic and ecological drivers of euphausiid community structure vary spatially in the Barents Sea: Relationships from a long time series (1952–2009). *Frontiers in Marine Science*, *1*. https://www.frontiersin.org/article/10.3389/fmars.2014.00074

Orlova, E., Rudneva, G., Renaud, P., Eiane, K., Savinov, V., & Yurko, A. (2010). Climate impacts on feeding and condition of capelin Mallotus villosus in the Barents Sea: Evidence and mechanisms from a 30 year data set. *Aquatic Biology - AQUAT BIOL*, *10*. https://doi.org/10.3354/ab00265

Osuga, D. T., & Feeney, R. E. (1978). Antifreeze glycoproteins from Arctic fish. *The Journal of Biological Chemistry*, *253*(15), 5338–5343.

Oziel, L., Sirven, J., & Gascard, J.-C. (2016). The Barents Sea frontal zones and water masses variability (1980–2011). *Ocean Science*, *12*(1), 169–184. https://doi.org/10.5194/os-12-169-2016

Pace, M. L., Cole, J. J., Carpenter, S. R., Kitchell, J. F., Pace, M. L., Cole, J. J., Carpenter, S. R., & Kitchell, J. F. (1999). Trophic cascades revealed in diverse ecosystems. *Trends in Ecology & Evolution*, *14*(12), 483–488. https://doi.org/10.1016/S0169-5347(99)01723-1

Perovich, D. K., Roesler, C. S., & Pegau, W. S. (1998). Variability in Arctic sea ice optical properties. *Journal of Geophysical Research: Oceans*, *103*(C1), 1193–1208. https://doi.org/10.1029/97JC01614

Raymont, J. E. G. (1983). In *Plankton and Productivity in the Oceans: Zooplankton* (2nd edition, p. 824). Pergamon Pr.

Reigstad, M., Carroll, J., Slagstad, D., Ellingsen, I., & Wassmann, P. (2011). Intra-regional comparison of productivity, carbon flux and ecosystem composition within the northern Barents Sea. *Progress in Oceanography*, *90*(1), 33–46. https://doi.org/10.1016/j.pocean.2011.02.005

Renaud, P., Berge, J., Varpe, Ø., Lønne, O., Nahrgang, J., Ottesen, C., & Hallanger, I. (2012). Is the poleward expansion by Atlantic cod and haddock threatening native polar cod, Boreogadus saida ? *Polar Biology*, *35*, 401–412. https://doi.org/10.1007/s00300-011-1085-z

Renaud, P. E., Daase, M., Banas, N. S., Gabrielsen, T. M., Søreide, J. E., Varpe, Ø., Cottier, F., Falk-Petersen, S., Halsband, C., Vogedes, D., Heggland, K., & Berge, J. (2018). Pelagic food-webs in a changing Arctic: A trait-based perspective suggests a mode of resilience. *ICES Journal of Marine Science*, *75*(6). https://doi.org/10.1093/icesjms/fsy063

Sagar, M., Nair, R., & Gop, A. (2019). *Stomach Content Analysis Techniques in Fishes*.

Sakshaug, E. (1997). Biomass and productivity distributions and their variability in the Barents Sea. *ICES Journal of Marine Science*, *54*(3), 341–350. https://doi.org/10.1006/jmsc.1996.0170

Sakshaug, E. (2004). Primary and Secondary Production in the Arctic Seas. In R. Stein & R. W. MacDonald (Eds.), *The Organic Carbon Cycle in the Arctic Ocean* (pp. 57–81). Springer. https://doi.org/10.1007/978-3-642-18912-8_3

Sakshaug, E., Bjørge, A., Gulliksen, B., Loeng, H., & Mehlum, F. (1994). Structure, biomass distribution, and energetics of the pelagic ecosystem in the Barents Sea: A synopsis. *Polar Biology*, *14*(6), 405–411. https://doi.org/10.1007/BF00240261

Sakshaug, E., Johnsen, G. H., & Kovacs, K. M. (2009). *Ecosystem Barents Sea*. Tapir Academic Press.

Sakshaug, E., & Slagstad, D. (1992). Sea ice and wind: Effects on primary productivity in the Barents Sea. *Atmosphere-Ocean*, *30*(4), 579–591. https://doi.org/10.1080/07055900.1992.9649456

Samemoto, D. D. (1987). Vertical distribution and ecological significance of chaetognaths in the Arctic environment of Baffin Bay. *Polar Biology*, *7*(6), 317–328. https://doi.org/10.1007/BF00293222

Scott, C. L., Falk-Petersen, S., Sargent, J. R., Hop, H., Lønne, O. J., & Poltermann, M. (1999). Lipids and trophic interactions of ice fauna and pelagic zooplankton in the marginal ice zone of the Barents Sea. *Polar Biology*, *21*(2), 65–70. https://doi.org/10.1007/s003000050335

Scott, C. L., Kwasniewski, S., Falk-Petersen, S., & Sargent, J. R. (2000). Lipids and life strategies of Calanus finmarchicus, Calanus glacialis and Calanus hyperboreus in late autumn, Kongsfjorden, Svalbard. *Polar Biology*, *23*(7), 510–516. https://doi.org/10.1007/s003000000114

Skjoldal, H. R., Gjøsæter, H., & Loeng, H. (1992). The Barents Sea ecosystem in the 1980s: Ocean climate, plankton, and capelin growth. *ICES Marine Science Symposia*, *195*, 278–290.

Skjoldal, H. R., Hassel, A., Rey, F., & Loeng, H. (1987). *Spring phytoplankton development and zooplankton reproduction in the central Barents Sea in the period 1979-1984*. https://imr.brage.unit.no/imr-xmlui/handle/11250/107832

Slagstad, D., Ellingsen, I. H., & Wassmann, P. (2011). Evaluating primary and secondary production in an Arctic Ocean void of summer sea ice: An experimental simulation approach. *Progress in Oceanography*, *90*(1), 117–131. https://doi.org/10.1016/j.pocean.2011.02.009

Smoot, C., & Hopcroft, R. (2017). Depth-stratified community structure of Beaufort Sea slope zooplankton and its relations to water masses. *Journal of Plankton Research*, *39*, 79–91. https://doi.org/10.1093/plankt/fbw087

Søreide, J. E., Hop, H., Carroll, M. L., Falk-Petersen, S., & Hegseth, E. N. (2006). Seasonal food web structures and sympagic–pelagic coupling in the European Arctic revealed by stable isotopes and a two-source food web model. *Progress in Oceanography*, *71*(1), 59–87. https://doi.org/10.1016/j.pocean.2006.06.001

Søreide, J. E., Leu, E., Berge, J., Graeve, M., & Falk-Petersen, S. (2010). Timing of blooms, algal food quality and Calanus glacialis reproduction and growth in a changing Arctic. *Global Change Biology*, *16*(11), 3154–3163. https://doi.org/10.1111/j.1365-2486.2010.02175.x

Søreide, J., Hop, H., Falk-Petersen, S., Gulliksen, B., & Hansen, E. (2003). Macrozooplankton communities and environmental variables in the Barents Sea marginal ice zone in late winter and spring. *Marine Ecology Progress Series*, *263*, 43–64. https://doi.org/10.3354/meps263043

Sunday, J. M., Bates, A. E., & Dulvy, N. K. (2012). Thermal tolerance and the global redistribution of animals. *Nature Climate Change*, *2*(9), 686–690. https://doi.org/10.1038/nclimate1539

Tande, K. S. (1991). Calanus in North Norwegian fjords and in the Barents Sea. *Polar Research*, *10*(2), 389–408. https://doi.org/10.3402/polar.v10i2.6754

Trudnowska, E., Gluchowska, M., Beszczynska-Moeller, A., Blachowiak-Samolyk, K., & Kwasniewski, S. (2016). Plankton patchiness in the Polar Front region of the West Spitsbergen Shelf. *Marine Ecology Progress Series*, *560*. https://doi.org/10.3354/meps11925

Våge, S., Basedow, S., Tande, K. S., & Zhou, M. (2014). Physical structure of the Barents Sea Polar Front near Storbanken in August 2007. *Journal of Marine Systems*, *130*, 256–262. https://doi.org/10.1016/j.jmarsys.2011.11.019

Vinje, T. (2009). Sea-ice. In *Ecosystem Barents Sea* (pp. 65–82). Tapir Academic Press.

Wassmann, P., Reigstad, M., Haug, T., Rudels, B., Carroll, M. L., Hop, H., Gabrielsen, G. W., Falk-Petersen, S., Denisenko, S. G., Arashkevich, E., Slagstad, D., & Pavlova, O. (2006). Food webs and carbon flux in the Barents Sea. *Progress in Oceanography*, *71*(2), 232–287. https://doi.org/10.1016/j.pocean.2006.10.003

Wassmann, P., Slagstad, D., & Ellingsen, I. (2019). Advection of Mesozooplankton Into the Northern Svalbard Shelf Region. *Frontiers in Marine Science*, *6*. https://www.frontiersin.org/article/10.3389/fmars.2019.00458

Welch, H. E., Crawford, R. E., & Hop, H. (1993). Occurrence of Arctic Cod (*Boreogadus saida*) Schools and Their Vulnerability to Predation in the Canadian High Arctic. *ARCTIC*, *46*(4), 331–339. https://doi.org/10.14430/arctic1361

Yaragina, N. A., & Dolgov, A. V. (2009). Ecosystem structure and resilience—A comparison between the Norwegian and the Barents Sea. *Deep Sea Research Part II: Topical Studies in Oceanography*, *56*(21), 2141–2153. https://doi.org/10.1016/j.dsr2.2008.11.025

Zhukova, N., Nesterova, V., Prokopchuk, I., & Rudneva, G. (2009). Winter distribution of euphausiids (Euphausiacea) in the Barents Sea (2000-2005). *Deep-Sea Research Part Ii-Topical Studies in Oceanography - DEEP-SEA RES PT II-TOP ST OCE*, *56*, 1959–1967. https://doi.org/10.1016/j.dsr.2008.11.007

APPENDIX I

Ice Categories

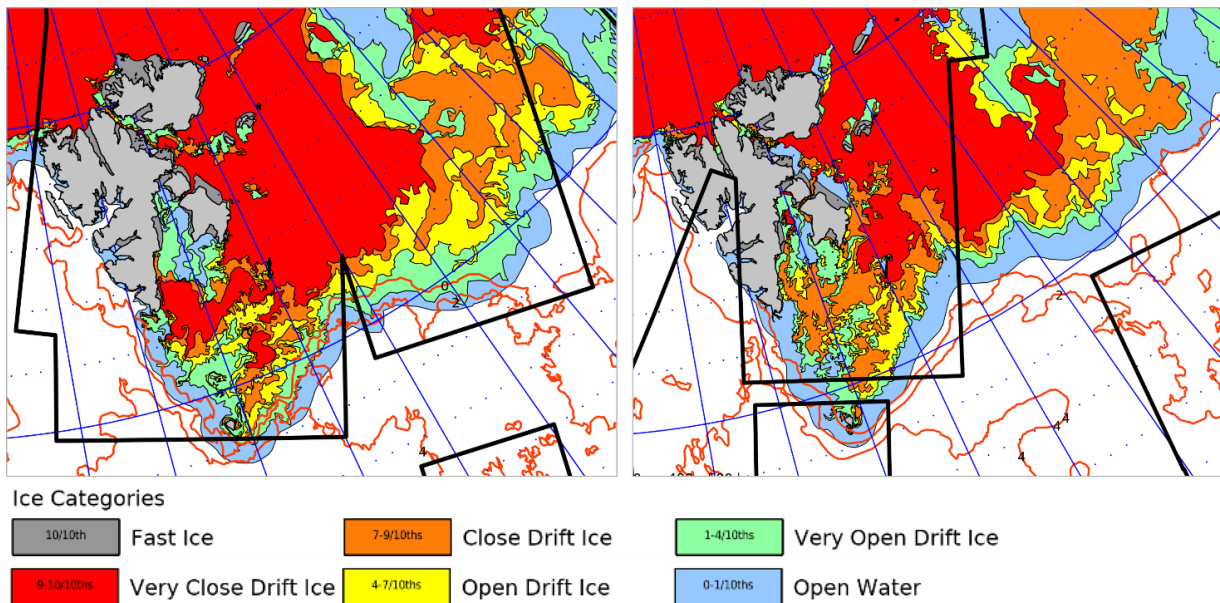|			
10/10th Fast Ice	7-9/10ths Close Drift Ice	1-4/10ths Very Open Drift Ice	
9-10/10ths Very Close Drift Ice	4-7/10ths Open Drift Ice	0-1/10ths Open Water	

Figure 19: *Ice charts on 2022-05-19 (left) and 2022-05-23 (right). Colors correspond to the sea-ice thickness.*

Measuring beta diversity

Beta diversity, which compares species assemblage among sites, can be measured through differences in richness and species replacement, and was described in detail by Legendre (2014). Where some sites may be characterized by richness differences, others may be dominated by differences in species composition. Local site contribution to the beta diversity can also be calculated to find significant differences among sites, and these can be related to ecosystem processes to can give indications of ecosystem functioning. In this study, presence-absence data of species collected from Tucker trawl samples were used to calculate the beta diversity across the PF stations using the Jaccard index. Despite PF3 being ecologically significant in terms of species abundance (the catch was close to empty), it was excluded from the analysis for the purpose of comparing species composition in relationship to the different water masses. Higher Jaccard values can be interpreted as sites being more dissimilar to others. PF6 was significantly different from the rest of the stations (p = 0.004), while the overall beta diversity could mostly be explained by a proportional difference in species richness (60.9%) and to a lesser extent by species replacement (39.1%). Local station contribution indicated that PF6 had the highest proportion of species replacement (39.1%), whereas PF4 contributed mostly to species richness (42.8%).

Stomach content analysis methodologies

Different methodologies on stomach content analysis of fish have been analysed and reviewed by various authors, including Buckland et al., 2017; Amundsen & Sánchez-Hernández, 2019; and V Sagar et al., 2019. The following content provides an overview of advantages and disadvantages of frequently used methodologies based on the papers mentioned above (see next page).

Table 4: *overview of frequently used stomach content analysis methodologies*

Method	Description	Advantages	Disadvantages
Frequency-occurrence	Also known as presence-absence method; relies on the positive identification of a(n identifiable part of the) prey in the diet	Quick, easy, and cost-efficient for determining diversity and prey taxa in the diet Most robust measurement of diet composition	No information on quantitative prey importance in terms of relative contribution to overall food quantity May lead to overestimation of small prey and prey that are part of general feeding strategies (prey with high frequencies but low abundance) May overestimate the importance of incidental prey and prey that are slow or resistant to digestion (e.g. prey with large exoskeletons)
Numerical	Based on the prey item counts present in the stomachs, expressed as a frequency of the total number of prey individuals/categories.	Useful in prey selectivity studies, provides information on the dietary composition Suitable for quantification of relative prey importance Often applicable to planktivorous and benthivorous fish	Requires that prey items are easily identifiable and counted, so not too heavily digested Outcome is meaningless if the prey largely varies in size (e.g. copepods vs. fish) May overestimate the importance of small prey items when consumed in large quantities*

*However, many fish have size-selective feeding strategies

Method	Description	Advantages	Disadvantages
Gravimetric	In gravimetric (weight-based) analysis of stomach contents in wet or dry weight. The relative prey contribution is expressed as a fraction of the total weight of prey.	Provides the finest resolution and precision on dietary composition and prey diversity Most suitable when the objective is to quantify food and energy consumption Suitable when prey taxa need to be categorized in relatively few groups with different digestion rates Taking bulk weight of grouped prey may be easier than counting numerous individual prey items	Time-consuming if many prey individuals need to weigh separately Highly digested prey items or prey covered in mucus can be difficult to separate from each other, and can affect weight measurements A high precision may not always reflect the diet composition accurately May overestimate the importance of prey with slow digestion rates*
Reconstruction	Back-calculations of the original prey item weight (based on size measurements of undigested prey item remains) are used to estimate relative prey importance and dietary composition.	The most robust and reliable approach if the objective is to quantify the relative diet composition in terms of biomass flow Prey items with high digestion rates regain their importance from back-calculations	Very laborious Datasets on weight of each prey taxon are often not available Small indigestible or slowly digestible prey items that remain in the stomach for longer time periods may be overestimated due to back-calculations to original prey weight.
Volumetric	The volumetric method provides bulk measurements of prey and uses volume (e.g. by measuring liquid displacement).	Suitable for large prey items	Less suitable for highly digested or small prey items like zooplankton Mucus may prevent prey from being separated Laborious and time consuming

*considering consumption rates can increase accuracy on estimation of the relative contribution of each prey type

Method	Description	Advantages	Disadvantages
Point	The point method ranks prey items in the stomachs on a chosen scale (common, rare, etc.) using points in proportion to their estimated dietary contribution.	Simple and fast, suitable for large sample sizes	Often subjective, outcome can vary considerably Approximate relative to the numerical and gravimetric methods
Relative-fullness	The relative-fullness method visually scores the relative prey contribution in terms of volume to the total stomach content. The total fullness of all stomach contents is first visually assessed usually on a scale from empty (0%) to full (100%).	Simple and fast, applicable to large sample sizes Provides a robust overview of the relative diet when executed carefully In combination with the frequency occurrence method, it provides the most quick and robust results	Often subjective and low precision of measurements* An estimate to the numerical and gravimetric methods
DNA-based	Uses DNA sampled from the stomachs to identify prey items in a semi-quantitative manner	Provides high taxonomic resolution of prey Combined with visual methods becomes a powerful tool Suitable for prey that digests quickly or prey that is difficult to visually detect/identify by species taxon (e.g. prey with large volumes of water, small indistinguishable species)	sequencing data often not available in public gene databases DNA may already be degraded during the digestion process Results are limited to frequency-occurrence and species richness due to the semi-quantitative nature of the analysis Secondary prey (prey consumed by the primary prey) may lead to overestimation of the richness

*However, blind-tests showed no significant differences between trained and untrained people

APPENDIX II

Supplementary results

Labels in image:
- *Hyperoche medusarum*
- *Boreogadus saida* larva
- *Paraeuchaeta norvegica*
- *Gelatinous zooplankton*
- Fish egg
- *Chaetognaths*
- Copepod soup (PF6)
- *Thysanoessa inermis*
- *Clione limacina*
- *Themisto libellula*
- Photos: Frida Cnossen
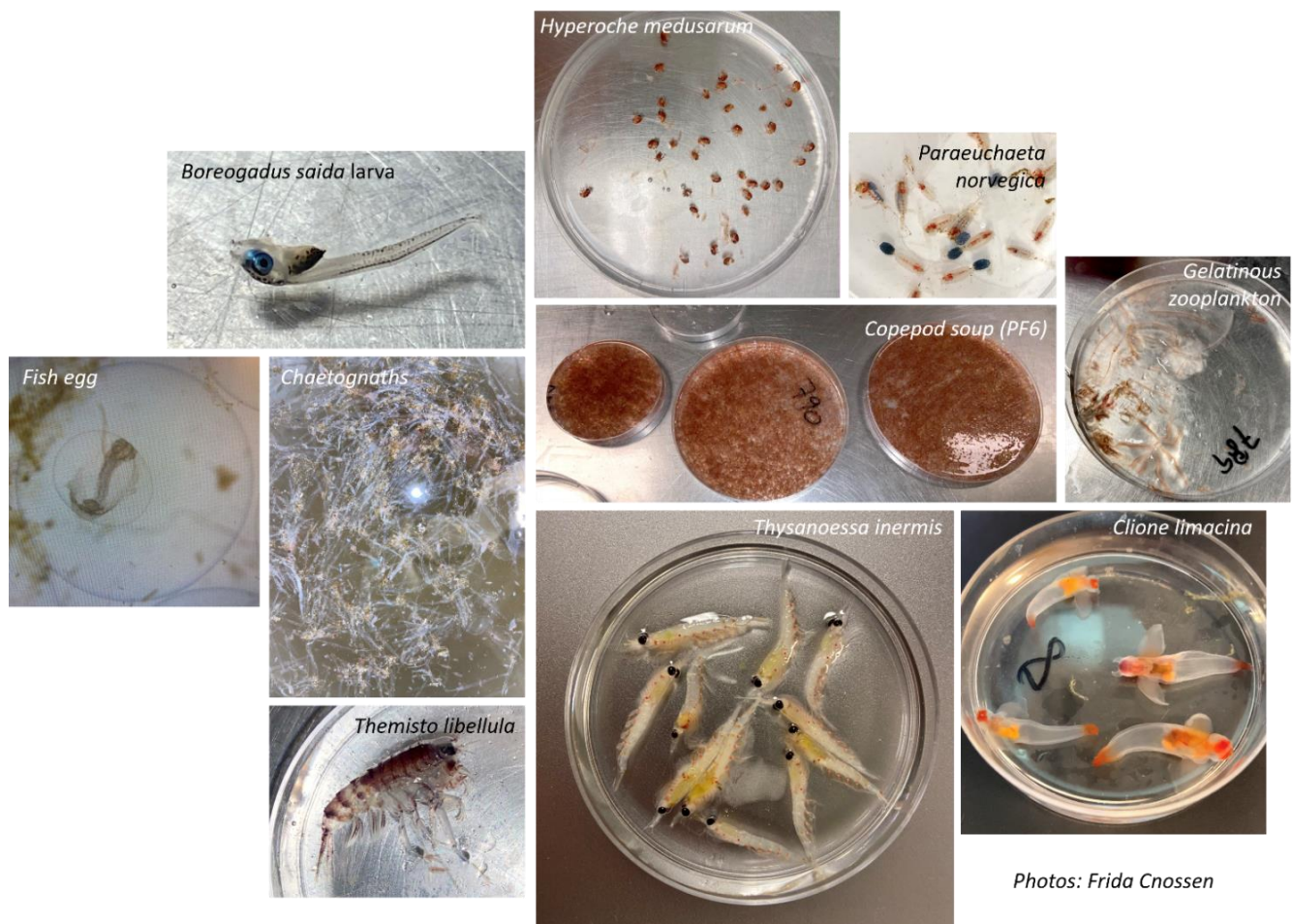
***Figure 20**: zooplankton catch overview (combined pictures from several trawls)*

Labels in image:
- 0 m
- Depth (m)
- Capelin schools
- Scattered capelin
- 18 kHz
- Sv (dB re 1 m⁻¹)
- -90
- -40
- 300 m
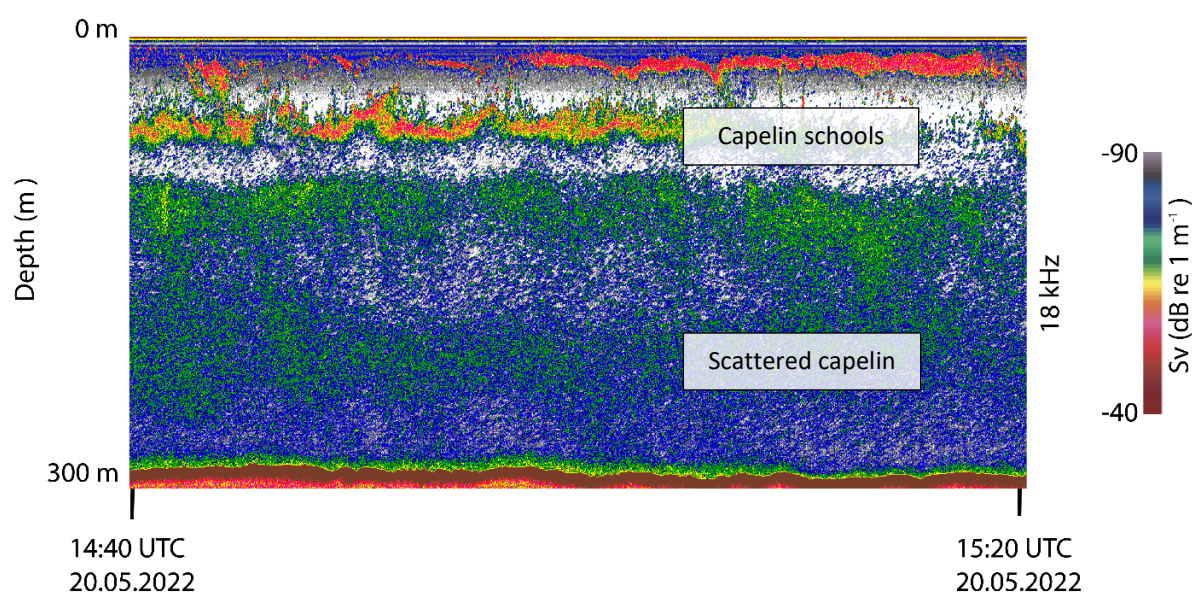- 14:40 UTC 20.05.2022
- 15:20 UTC 20.05.2022

***Figure 21**. Example of a hull-mounted EK60 echogram at 18 kHz on 20 May, 2022.*

Table 5: *macrozooplankton species with corresponding distribution, feeding mode, and occurrence per station and water mass. Taxa are grouped by zoogeographical (zoogeo.) region (a: Arctic, ab: Arctic-boreal, ba: boreal-Arctic, c: cosmopolitan, u: unknown) and feeding mode (h: herbivorous, o: omnivorous, c: carnivorous, u: unknown). Stations are grouped by water mass (AW: Atlantic Water and ArW: Arctic Water). x indicates presence of a species at a given station. Sources: [1]Søreide et al., 2003 [2]Dalpadado et al., 2008 [3]Smoot & Hopcroft, 2017 [4]Legeżyńska et al., 2017 [5]Bluhm et al., 2017 [6]Cairns et al., 2002 [7]Aune et al., 2021.*

Taxon	Zoogeo.	Feeding	PF1	PF2	PF3	PF4	PF5	PF6	
Amphipoda									
Themisto libellula[1,2]	a	c					x	x	
Themisto abyssorum[1,2]	ab	c					x		
Hyperoche medusarum[3,4]	ab	c					x		
Apherusa glacialis[3,5]	a	o				x			
Chaetognatha									
Parasagitta elegans[1,3]	ab	c	x	x	x	x	x	x	
Eukrohnia hamata[1,3]	c	c	x	x		x	x		
Cnidaria									
Aglantha digitale[1]	ab	c	x			x	x		
Euphysa flamea[6]	ab	c					x		
Copepoda									
Calanus finmarchicus[1]	ba	h	x	x	x	x	x	x	*
Calanus glacialis[1,3]	a	h	x	x		x	x	x	*
Calanus hyperboreus[1,3]	a	h	x	x	x	x	x	x	*
Metridia longa[3]	ab	o	x	x	x	x	x		
Paraeuchaeta norvegica[1]	ab	c	x			x			
Ctenophora									
Beroe cucumis[1]	ab	c	x			x	x	x	
Decapoda									
indet.	u	u				x	x		
Euphausiidae									
Thysanoessa inermis[1,2,3]	ba	h	x	x		x	x	x	
Thysanoessa longicaudata[1,2]	ba	o	x	x		x	x	x	
Meganyctiphanes norvegica[1,2]	b	o	x			x			
Mysidacea									
indet.	u	u				x			
Siphonophora									
indet.	u	u					x		
Pteropoda									
Clione limacina[1,3]	ab	c			x	x		x	
Limacina helicina[1,3]	ab	o					x		
Vertebrata									
Boreogadus saida larvae[7]	a	o						x	
Fish eggs (indet.)	u	u	x	x	x	x			

*based upon species identification from multinet sampling
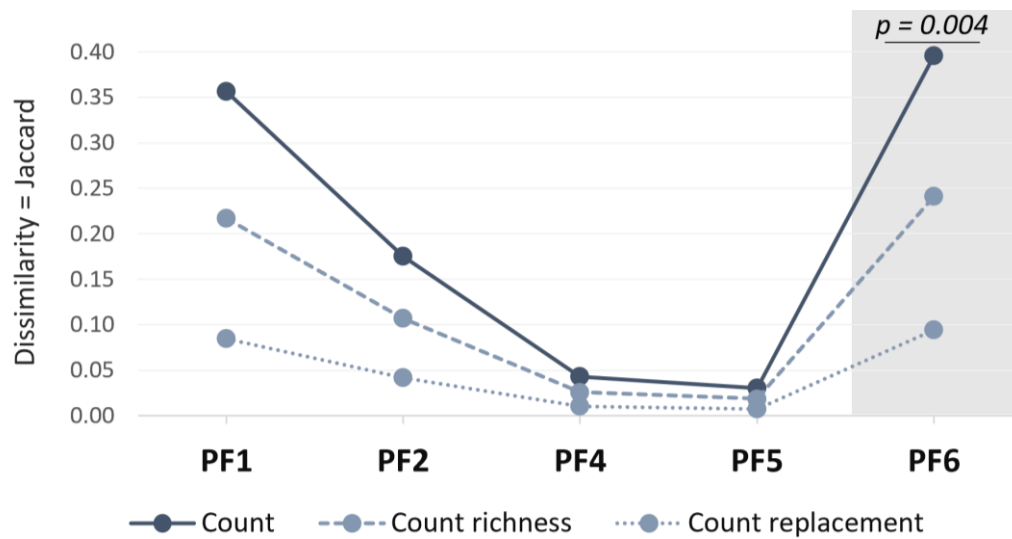
Figure 22: *Betadiversity of macrozooplankton count among sites, expressed in Jaccard dissimilarity values and proportional contribution of richness difference and species replacement. Despite PF3 likely being ecological significant in terms of species abundance (the catch was close to empty), it was excluded from the analysis for the purpose of comparing species composition in relationship to the different water masses. Higher values indicate greater dissimilarity, and vice versa.*